Ultraviolet Dosage and Decontamination Efficacy was Widely Variable Across 14 UV Devices after Testing a Dried Enveloped Ribonucleic Acid Virus Surrogate for SARS-CoV-2

Running title: UV Decontamination, Enveloped Virus

Tony L. Buhr[1], Erica Borgers-Klonkowski[1], Bradford W. Gutting[1], Emlyn E. Hammer[1], Shelia M. Hamilton[1], Brett M. Huhman[2], Stuart L. Jackson[2], Neil L. Kennihan[1], Samuel D. Lilly[1], John D. Little, Jr[2], Brooke B. Luck[1], Emily A. Matuczinski[1], Charles T. Miller[1], Rachel E. Sides[1], Vanessa L. Yates[1], Alice A. Young[1]

[1]Naval Surface Warfare Center-Dahlgren Division, Concepts and Experimentation Branch (B64), Dahlgren, VA USA

[2]Naval Research Laboratory (Plasma Physics Division), Washington, DC USA

Correspondence:
Tony L. Buhr, PhD
tony.l.buhr.civ@us.navy.mil

Keywords: Φ6, enveloped virus, decontamination, ultraviolet (UV), SARS-CoV-2, COVID19

Abstract

Aims: The dosages and efficacy of 14 ultraviolet (UV) decontamination technologies were measured against a SARS-CoV-2 surrogate virus that was dried on to different materials for lab and field testing.

Methods and Results: A live enveloped, ribonucleic acid virus surrogate for SARS-CoV-2 was dried on stainless steel 304 (SS304), Navy Top Coat-painted SS304 (NTC), cardboard, polyurethane, polymethyl methacrylate (PMMA), and acrylonitrile butadiene styrene (ABS) at > 8.0 $\log_{10}$ plaque-forming units (PFU) per test coupon. The coupons were then exposed to UV light during both lab and field testing. Commercial and prototype UV-emitting devices were measured for efficacy; 4 handheld devices, 3 room/surface-disinfecting machines, 5 air-disinfection devices, and 2 larger custom-made machines. UV device dosages ranged from 0.01-729 mJ cm^{-2}. Anti-viral efficacy among the different UV devices ranged from no decontamination up to nearly achieving sterilization. Importantly, cardboard required far more dosage than SS304.

Conclusions: Enormous variability in dosage and efficacy was measured among the different UV devices. Porous materials limit the utility of UV decontamination.

Significance and Impact of the Study: UV devices have wide variability in dosages, efficacy, hazards, and UV output over time indicating that each UV device needs independent technical measurement and assessment for product development, and prior to use.

INTRODUCTION

UV light, particularly UV-C, is a known microbe disinfectant for air, water and nonporous surfaces (Anonymous 2021a, Anonymous 2021b). UV-C radiation can only inactivate microbes including viruses if they are directly exposed to the UV light. Therefore inactivation is far less effective if a microbe is associated with soil, dust, oils, any type of host cell debris, or if it is embedded in porous materials (Anonymous 2021a). This is particularly relevant for obligate pathogens like viruses which are naturally associated with host cell components and body fluids; mucus in the case of respiratory virus like SARS-CoV-2 (Stadnytskyi et al. 2020). The effectiveness of UV-C lamps in inactivating environmentally relevant SARS-CoV-2 virus is unknown because there is limited consistent and/or reliable published data about the wavelength, dose, and duration of UV-C radiation required to inactivate the SARS-CoV-2 virus (Anonymous 2021a; Anonymous 2021b). This is true of all viruses because UV efficacy is further complicated by the fact that test methods for virus preparation and testing, particularly enveloped viruses, are highly variable among laboratories. Purified enveloped viruses are often tested in laboratories, even though these viruses only exist naturally when associated with host cell components and debris in nature, and they can be compromised during purification. For example, hemagglutinin stabilizes influenza A (Russell 2021) and mucus stabilizes SARS-CoV-2 (Stadnytskyi et al. 2020), but both are typically absent from laboratory virus preparations. These stabilizing components can be added to virus, but often are not added, and there are other host cell components that may act as stabilizers as well. Furthermore, based on published measurements, SARS-CoV-2 respiratory droplets are typically 0-1 virions per speech particle, 99.9875-99.9998% mucus, less than 0.013% virus, and the water in SARS-CoV-2 respiratory particles evaporates within seconds to generate dry particles in the respirable size range (Stadnytskyi et al. 2020). Enveloped virus is more stable at dry conditions compared to wet environments (Chan et al. 2011; Buhr et al. 2020; Hadi et al. 2020), and drying viruses via lyophilization is frequently used to stabilize virus for long-term storage (Greiff et al. 1954; Greiff and Richtel 1966; Malenovska 2014). Hence tests on wet virus vice dry virus will also greatly impact decontamination kinetics. Rhinotillexis (nose-picking) creates additional environmental loads of infectious virus, which is also composed of mucus mixed with unpurifed virus, and varying levels of free water (Hendley et al. 1973; Weber et al. 2008).

In addition to methods gaps to define, characterize and standardize SARS-CoV-2 virus debris composition and drying, standardized methods for reproducibly preparing large titers of SARS-CoV-2 for testing without artificial post-harvest cleaning and concentration steps are needed. Furthermore, there were/are urgent needs during the COVID-19 pandemic to test decontamination devices, like UV, in field tests (any test outside of biosafety containment).

Viruses that fall under higher World Health Organization (WHO) biosafety level (BSL) classifications such as SARS-CoV-2 (BSL-3) and its BSL-2 surrogate coronaviruses (Anonymous 2020) cannot be widely used in field tests because of cost, time, and safety constraints. For field testing, the enveloped virus surrogate Φ6 (Bibby et al. 2015; Gallandat and Lantagne 2017; Fedorenko et al. 2020) was previously used to make live/dead Φ6 test indicators to directly test and compare decontamination efficacy across lab and field tests (Buhr et al. 2020).

Pseudomonas virus Φ6 is a BSL-1 enveloped RNA virus originally isolated in a bean field as a lytic virus that infects the plant pathogenic bacterium *Pseudomonas syringae* pathovar *phaseolicola* (Vidaver et al. 1973; Van Etten et al. 1976; Mindich 2004). The Φ6 envelope structure is similar to many other enveloped viruses as the envelope consists of a glycoprotein/protein-embedded lipid membrane and the host cell has similar temperature sensitivity to mammalian cells at around 40°C. This is important since the envelope components are considered a target for inactivation by many different decontaminants including UV light, particularly at 222 nm (McDonnell and Burke 2011; Wiggington et al. 2012; Hadi et al. 2020; Anonymous 2021a). Φ6 is a 13.5 kb double-stranded (ds)RNA phage (Mindich 2004), and spherical (80-100 nm diameter) with structural similarity to coronaviruses (50-200 nm diameter). The 13.5 kb dsRNA genome, the equivalent of 27 kb of single stranded RNA (ssRNA), is comparable to the 26-32 kb of ssRNA in coronaviruses. In theory, a surrogate virus should have a similar number of adjacent pyrimidines compared to SARS-CoV-2 since pyrimidine dimerization is considered an important mechanism of UV inactivation (e.g. Heßling et al. 2020). Based on pyrimidine target numbers only, Φ6 (6,613 adjacent pyrimidine pairs) and SARS-CoV-2 (7,600 pairs) should have similar UV sensitivity, although ssRNA may be slightly more sensitive than dsRNA due to the potential for repair of dsRNA by the undamaged strand (Tseng and Li 2005). Hence sequence data alone theoretically implies that Φ6 inactivation goals should be similar to or slightly more conservative than SARS-CoV-2. Separately, it is currently difficult to compare UV efficacy both within and across different viruses based on existing data because experimental tests are highly variable across different labs and studies (Hadi et al. 2020). Overall, the sequence comparison between the two viruses is likely moot because debris, drying, and porosity of contaminated surfaces have dominant impacts on decontamination kinetics (Anonymous 2021a, Anonymous 2021b), and practical confidence that test methods approach the challenge of field conditions is needed from field testing in order to increase confidence in devices to be employed by end users.

The subject of decontamination using UV light has attracted tremendous attention during the COVID-19 pandemic (reviewed in Raiszadeh and Adeli 2020), and numerous products incorporating UV light sources are available on the market to decontaminate air, water and surface materials. Variability in UV devices is extensive and includes differences in electronics, bulbs, power, and product designs. Devices that incorporate UV lights include handheld devices, room decontamination devices and HVAC systems. The distance from light sources at which decontamination/inactivation occurs is also widely variable ranging from a couple of centimeters to a couple of meters. UV light sources also differ and include mercury (Hg), Krypton Chloride (KrCl), Xenon (Xe) and various light emitting diodes (LED), which range in wavelength, and there are several different manufacturers. Additionally, although Hg bulbs are the most common, Hg bulb dosage significantly varies over time after the Hg bulb is turned on, and Hg comes with the risk of toxicity. The variability in these decontamination devices is further complicated by

variability in test methods which include different virus preparation methods, tests with unpurified vs. purified virus, tests with wet virus or dried virus, presence of organic debris, and differences in porosity of surface materials. Assessments of UV for decontamination must also take into account maintenance since UV lights need to be cleaned in order to maintain dosage (Anonymous 2021a, Anonymous 2021b).

Here Φ6 was prepared at >10 $\log_{10}$ PFU ml^{-1} without post-harvest processing or concentration steps, and then dried on to different materials for >24 hours (h) to make BSL-1 live/dead enveloped virus test indicators at ≥ 8.0 $\log_{10}$ PFU $coupon^{-1}$. Numerous UV devices were tested in both lab and field trials for both screening and iterative UV product improvement.

MATERIALS AND METHODS

Φ6 and Host Cell Preparations

Virus and host cell preparation was previously described (Buhr et al. 2020). Φ6 and its host organism *P. syringae* pathovar *phaseolicola* HB10Y (HB10Y), causal agent of halo blight of the common bean, *Phaseolus vulgaris*, were isolated in Spain. Both were a kind gift from Dr. Leonard Mindich at Rutgers University, New Jersey Medical School. HB10Y was prepared by inoculating 100-200 ml of 3% tryptic soy broth (TSB; Fluka PN#T8907-1KG) in a 1-liter (l) smooth-bottom Erlenmeyer flask with a high efficiency particulate air filter cap. Cultures were incubated at 26±2°C, 200 revolutions (rev) minute $(min)^{-1}$ for 20±2 h. 11.1 ml of 100% glycerol (Sigma PN #G7757-500ML) was added per 100 ml of host culture. Final concentration of glycerol was 10%. One-ml aliquots of HB10Y were pipetted into screw-cap microfuge tubes with O-rings, and stored at -80°C. HB10Y samples were titered prior to freezing by serially diluting samples in 10 millimolar (mM) of 4-(2-hydroxyethyl)-1-piperazineethanesulfonic acid (HEPES, Sigma PN#H4034-100G) + 10% Sucrose (Sigma PN #S7903-250G), pH 7.0, and plating on tryptic soy agar (TSA; Hardy Diagnostics, Santa Maria, CA). Plates were inverted and incubated at 26±2°C for 48±2 h to show titers of ~10^9 cells ml^{-1}. After freezing, tubes were thawed at room temperature (RT, 22±3°C), serially diluted and plated to show sustained viability after long-term storage at -80°C.

Φ6 was prepared after inoculating broth cultures of HB10Y. A frozen stock prep of HB10Y was thawed at 22±3°C. HB10Y was added either directly from a frozen stock or by transferring a single colony from a streaked TSA plate to 200 ml of 3% TSB in a 1-l smooth-bottom Erlenmeyer flask with a HEPA cap and incubated at 26±2°C, 200 rev min^{-1} overnight. Cells were then diluted and grown to mid-log-phase. The host flask was inoculated with 0.5-1 ml of Φ6 at a stock concentration of ~11-12 $\log_{10}$ PFU ml^{-1}. The culture was incubated at 26±2°C, 200 rev min^{-1} for 24±2 h. The Φ6 preparation was stored at 4°C until after titering was completed. After titer determination was completed, typically around 11-12 $\log_{10}$ PFU ml^{-1}, then 1-1.3 ml volumes were aliquoted into 1.5-ml screw-cap tubes with O-rings, inverted and stored at -80°C.

Coupon Materials and Sterilization

2 centimeter (cm) x 2 cm coupons of different test materials were inoculated with ≥8.0 $\log_{10}$ PFU Φ6 virus inoculum (Buhr et al. 2020). Materials for inoculation included stainless steel 304 (SS304), SS304 coupons painted with Navy Top Coat (NTC) (Coatings Group at the University of Dayton Research Institute (Dayton, OH, USA), acrylonitrile butadiene styrene (ABS) plastic, polymethyl methacrylate (PMMA) plastic (keyboard keys from Hewlett-Packard computer keyboards, later replaced with ABS), polyurethane plastic and cardboard. Plastic and SS304 represent non-porous materials. NTC represent semi-porous surfaces found on military ships. Cardboard represents porous materials used in shipping although it is not considered as porous as fabrics or carpeting.

For sterilization, SS304 and NTC coupons were rinsed with 18 mega-Ohm-cm, de-ionized water, placed on absorbent paper in an autoclave-safe container and autoclaved for 30 min at 121ºC, 100 kilopascals. Keyboard keys were removed, trimmed, cleaned with soap, then rinsed with de-ionized water and wrapped in aluminum foil. ABS coupons were similarly rinsed with de-ionized water and wrapped in foil. Cardboard coupons were devoid of noticeable debris, flaws, and ink, and were wrapped in foil. After wrapping in foil, the keyboard keys, ABS, and cardboard were all sterilized via hot, humid air at 95ºC and 90% relative humidity (RH) for 4 h. Polyurethane coupons, having been pre-cut, were soaked in ethanol to remove ink residue left over from the cutting process. They were then rinsed with de-ionized water, sterilized via immersion in 70% ethanol for greater than 20 min, and allowed to dry. All sterilized coupons were stored in sterile containers until used.

Coupon Inoculation and General Test Design

Five independent preparations of Φ6 were removed from -80°C storage and thawed at 22±3°C. Working inoculum was prepared by transferring stock Φ6 into 50-ml conical tubes containing 10mM HEPES + 10% Sucrose pH 7.0 with a final concentration of ~9 $\log_{10}$ PFU ml^{-1}. Coupons were inoculated with 0.1 ml of Φ6 working inoculum, and subsequently held at 22±3°C for greater than 24 h to dry and adhere to the material. The keyboard keys were slightly slanted. Therefore, during inoculation and drying, the keys were positioned in a sterilized surface which was elevated on an incline via slats to provide a level inoculation surface.

Once the inoculum had dried onto the coupons, they were exposed to UV light from the candidate devices as described in the below sections. Specific parameters for testing the individual devices varied but coupon number and preparation prior to testing was maintained across all experiments. For each test, five individual coupons were included for each of the test materials (SS304, cardboard, NTC, polyurethane, and either keyboard keys or ABS plastic), each inoculated with one of five independent virus preparations as described above. Extraction and shipping control coupons (inoculated and transported, when necessary, to the testing sites but not exposed to UV light) as well as negative control coupons not inoculated with virus were also included for every experiment. Finally, the Φ6 virus inoculum used to prepare the coupons was maintained at RT from the date of coupon inoculation through the test and viral titer was measured at the conclusion of test exposures for each experiment. After UV exposure during testing, surviving virus was extracted and quantified as described below.

Spectroscopic Analysis Hardware and Calibration

The primary spectrometer used for this work is the Ocean Optics Maya 2000 Pro, which is capable of measuring optical spectra from 180 – 630 nm with an average bin size of 0.22 nm across the measurable spectrum. The distribution is not strictly linear, but can be specifically determined as necessary for data processing. The spectrometer was used with a fiber bundle (BFL200HS02), which incorporates seven Φ200-μm core fibers into a single high-OH package. This enables the measurement of sources with low output so the spectrometer can both retain a high signal-to-noise ratio and enable the use of a cosine corrector (CCSA2) for most measurements.

The Maya 2000 Pro spectrometer was calibrated using a Cathodeon R48 Deuterium Lamp, serial number CH5627. The spectral irradiance from this lamp is in units of $mW \bullet m^{-2} \bullet nm^{-1}$ in 5 nm intervals from 200 – 400 nm. To perform the calibration, the lamp is mounted vertically and positioned so that a horizontal line through the center of the area to be irradiated passes through the center of the lamp emission area, as well as perpendicular to the lamp window. The calibration refers to the spectral irradiance over an approximately 10 mm^2 area in a vertical plane located at a distance of 200 mm from the outside surface of the output window on the lamp. The lamp is operated from a 300-mA power supply, and must be operated continuously for 30 min prior to recording data on the spectrometer.

The spectrometer was mounted on an optical table, with a three-axis linear translation stage (Thorlabs LTS300) used to enable precision alignment between the spectrometer fiber sensor head and the source of interest. The three-axis system is capable of measuring a 300 mm x 300 mm x 300 mm volume with computer automation using a process-controlled script via the Thorlabs Kinesis software. The data acquisition software used National Instruments LabVIEW for all aspects except direct control of the translation stages. All of the data was written to a single Technical Data Management Streaming data file for post-processing, which enabled all of the measurements to have a common time base for analysis. Post-processing was accomplished with the Jupyter software environment, with discrete Python code blocks to allow for processing of specific sources as needed. The raw TDMS data file is loaded into a cache file on the processing server, and a series of factors and calibrations are applied to prepare the raw data for analysis. Static measurements are relatively simple, as the position is fixed and no further analysis is required. Sweeps in a two-dimensional space with the translation stages requires synchronization of the position with digital fiducial markers to construct an image of the measured plane at a given distance from the source.

Ultraviolet Devices and Testing

A focus of this work was to provide information for screening field devices and to provide feedback for iterative product improvement. Specific data for prototypes were deliberately omitted since all prototypes were in the process of iterative improvement.

Commercial handheld devices (18-watt, 35-watt)

Two commercial handheld devices were acquired and tested, each within a custom test apparatus. The first was the GermAwayUV 18W Handheld UV-C Surface Sanitizer (SKU 202110, bulb SKU 195317, CureUV, Delray Beach, FL, USA), a 120V/60Hz device containing two 12.7-cm long, U-shaped (Hg) UV bulbs emitting 254 nm UV-C light (**Figure 1A**). An average intensity of 7.61 mW cm^{-2} was measured within a decontamination footprint of 4.47 cm

x 5.39 cm at a 5-cm standoff distance from the bulb (heat map of UV coverage is shown in **Figure 1C**). The second device was the GermAwayUV Premier 35W Handheld UV-C Surface Sanitizer (PN14-110-800-100, EPA Product No. 94850-DV-6, CureUV, Delray Beach, FL, USA), 120V/60Hz handheld containing two Hg bulbs that emit 254 nm UV-C light, with reflective material positioned within the unit to enhance UV coverage (**Figure 1B**). The twin tube bulbs spanned a length of 22.5 cm. The 35W device provided an average intensity of 6.95 mW cm^{-2} at 5-cm standoff distance from the bulb (**Figure 1D**). The 35W handheld was later discovered to contain ineffective ballasts (P/N 14-110-800-100), which negatively impacted results.

For testing the two handheld devices, wooden holding chambers were constructed in which the devices could be placed to provide standardized exposures to test materials. They were designed to hold the UV source 5 cm above the surface of a test coupon, to prevent UV reflection, and to allow coupons to be inserted into the apparatus via a sliding tray for a specified time period of virus inactivation and then promptly removed (**Figure 1A and 1B**). The design of the chambers was the same for the two devices, and only varied in size to accommodate the different dimensions of each device. Because Hg bulbs require a warm-up time to generate consistent dosage, the devices were powered on 30 min prior to testing to warm up and remained powered on for the duration of the test. To prevent potential contamination, the test chambers and devices were wiped down with pH6.8-adjusted bleach prior to being positioned inside a biosafety cabinet (BSC) for testing.

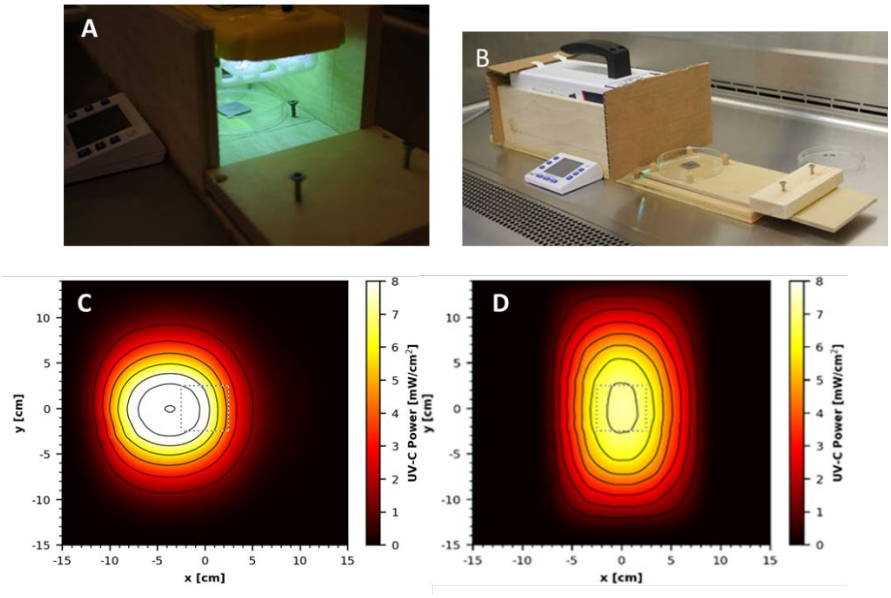

Figure 1. Testing setup and UV coverage for 18W and 35W handheld devices. **(A)** GermAwayUV 18W handheld device and custom test chamber, shown during a coupon exposure. **(B)** GermAwayUV 35W handheld device and custom test chamber, shown in the pre/post exposure state. **(C)** and **(D)** UV coverage heat maps for the 18W device **(C)** and the 35W device **(D)** taken 5 cm from the source.

The sliding tray was constructed to hold a sterile Petri dish via guides and included a stop bar to ensure that the sample would be consistently positioned directly under the center of the UV source for maximum exposure. A cardboard barrier was placed over the opening of the chamber to prevent premature UV exposure onto test coupons when the materials were outside the test chamber. The plastic lid was removed from the Petri dish prior to UV exposure and the dish was wide enough that the dish edges did not impede UV transmission.

A N=5 was tested for each material at each time point. Each of the 5 coupons was inoculated with an independent virus preparation, emphasizing statistical accuracy over precision, and 3 separate exposures were tested for a total N=15. Test chambers held the UV source at a distance of 5 cm from the coupons, with the exception of keyboard keys. The keyboard keys were taller and the distance from the UV bulb was 4.28-4.38 cm. The 18W and 35W handheld devices emitted steady state intensities of 10.12 mW cm^{-2} and 6.9 mW cm^{-2} respectively at the geometric center under the device. Test coupons were exposed to 10 or 20 seconds (s) of UV-C radiation from the 18W handheld and 2, 5, or 10 s of UV-C radiation from the 35W handheld. Different exposure times for the two devices were chosen based on pre-experimental predictions that were considered for practical application of the devices in a field setting. Prior to testing it was assumed that 35W radiation would exceed 18W and 10 s was a common time variable for both the 18W and 35W handhelds. During testing, the ambient environment was 22±2°C and 40% RH. The surface temperature within the test chamber reached 36°C under the 18W device and 48°C under the 35W device. Following UV exposure, coupons were transferred using sterile forceps to 50 ml conical tubes for extraction.

Prototype Handheld devices (272 nm LED and 222 nm Lamp Modules)

Two additional handheld devices were tested for efficacy of virus inactivation, which were prototypes rather than commercial units. The first prototype was one of two custom 3-D printed proprietary units and featured eight LED strips which emitted 272 nm wavelength UV-C light. The face of the handheld was 320 mm x 100 mm with the LED strips covering 255 mm x 60 mm. An average intensity of 12.71 mW cm^{-2} was measured within a decontamination footprint of 6 cm x 25.5 cm at 5 cm standoff distance from the bulb (**Figure 2A and 2B**). The second prototype device utilized three 222 nm UV-C Excimer Lamp Modules installed into a 2.54 cm thick white plastic panel with power supply. It is important to note that this was strictly an early prototype undergoing iterative improvements, and the UV sources were spaced too far apart for a wand configuration. An average intensity of 1.54 mW cm^{-2} was measured at 5 cm standoff distance from an individual module (**Figure 3A and 3B**).

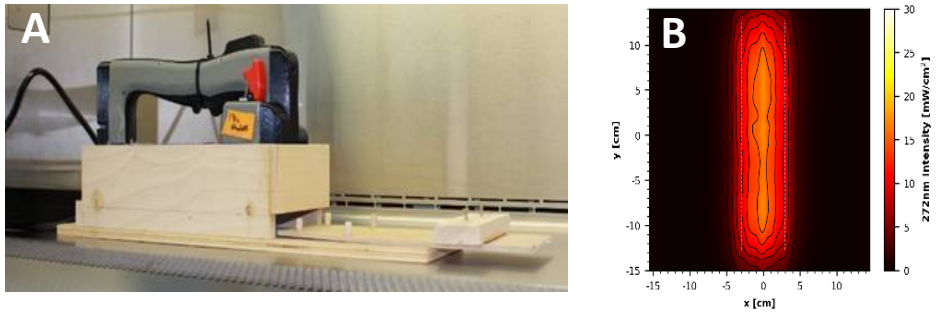

Figure 2. (A) Prototype 272 nm LED handheld inside wooden test chamber. **(B)** UV coverage heat map taken 5 cm from the source.

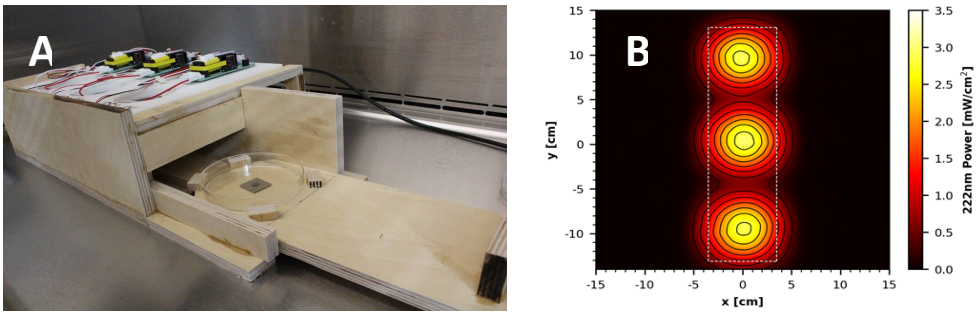

Figure 3. (A) Prototype 222 nm Excimer Lamp Module Board inside wooden test chamber. **(B)** UV coverage heat map taken 5 cm from the source.

The wooden test chambers for the prototype handhelds followed the same design as those for the 18W and 35W devices, with the additional feature of a wooden barrier that removed the need for cardboard to prevent premature UV exposure onto test coupons when the materials were outside the UV chamber. Again, there was a 5 cm vertical standoff distance from the UV light source to the surface of the test coupons. Mimicking the 18W and 35W handheld unit tests, the devices were powered on 30 min prior to testing to warm up and remained powered on for the duration of the test. An Ophir Spiricon Starbright Dosimeter (S/N 949685, P/N 7201580) and sensor (S/N 954282, P/N 7Z02479) were used to confirm that the 222 nm device was on and emitting 222 nm UV radiation, as the design of the prototype did not allow visual confirmation that the light was on after it was plugged in. The test chambers and handheld UV devices were wiped down with pH6.8-adjusted bleach prior to being positioned inside a BSC for testing.

A N=5 coupons for each material were tested at each time/dosage with each coupon inoculated with an independent virus preparation. During tests, virus-inoculated coupons were transferred singly to sterile Petri plates and inserted into the test chambers via the sliding tray for timed UV exposures at the geometric center of the handheld device. For the 272 nm device, the

cardboard coupons were anchored down using sterile pipette tips due to the large amount of air movement generated by the cooling fans of the device. In the 272 nm prototype, coupons were exposed to a steady state intensity of 15.6 mW cm^{-2} measured at the geometric center of the device with a 5 cm standoff distance. Similarly, the 222 nm prototype emitted an intensity of 2.96 mW cm^{-2} at a similar location centered under a single lamp module. Following UV exposure, the coupons were transferred to 50-ml conical tubes for extraction. For both devices, test coupons were exposed to UV-C radiation for 2, 5, or 10 s. For the 272 nm device, the ambient environment during testing was 21±2°C and 21% RH and the surface temperature under the sterilizer reached 34.7±2°C. For the 222 nm device, the ambient environment was 21.8±2°C and 20% RH and the surface temperature reached 28.3±2°C within the test chamber.

Prototype Mounted Pulsed Xe Unit for Room Decontamination

A prototype room-decontamination unit featuring a pulsed Xe UV bulb was tested. The unit consists of a pulsed Xe bulb within a frame intended to be mounted onto a wall, ceiling, or mobile tripod for room decontamination. The UV source emitted a small burst of broad-spectrum light every 6 s with the burst lasting for a short duration. The light spectrum included UV-C, UV-B, UV-A, and violet-blue light. Reflector material was positioned behind the source to enhance UV output.

Testing of the modified prototype took place within an enclosure provided by the vendor. The device was mounted at a 2-m, 1-m, and 0.5-m vertical standoff distance above the testing surface. Test coupons were placed below the prototype in sterile petri dishes and aseptic technique was employed to the greatest extent possible while outside of a BSC, to prevent contamination. The coupons contained within Petri dishes were uncovered just prior to the test and re-covered at the conclusion of the exposure times. Independent tests were run for 3 exposure times (15, 30, and 60 min), each taken at 0.5-m, 1-m, and 2-m distances from the UV source. These time increments were determined via the recommended cycle lengths from the vendor and corresponded to vendor test data (30 and 60 min only). The device was pre-programmed for 30 min run times, therefore for the 15-min increment, coupons were removed from the enclosure without shutting off the device after 15 min had elapsed from the time of the first flash. For the 60-min cycle, two decontamination cycles were run sequentially.

Commercial Rolling Units for Room Decontamination

Two commercial rolling units designed for room decontamination were purchased. The first was the Xenex Lightstrike (Model PXUV4D, S/N 002628, Xenex Disinfection Systems, San Antonio, TX, USA), which contained one pulsed Xe bulb (broad spectrum across the germicidal spectrum of 200-315 nm), which extends and retracts at the top of the unit and pulsed at a rate of 67 flashes per s. An average intensity of 0.02 mW cm^{-2} was measured at a 1.78 m standoff distance from the bulb, but intensities and dosages at specific wavelengths were not carefully analyzed/dissected since this work was not aimed at correlating specific wavelength dosages within a broad spectrum to kill. The second unit was the Light Emitting Module ("LEM," Rapid UV-C Disinfection Model R3, S/N 473, 120V/12A, STERILIZ, LLC, 150 Linden Oaks, Rochester, NY 14625-2802), which contained a ring of twenty Hg bulbs with a 41-cm diameter that emitted predominantly 254 nm wavelength UV-C light. The device was tested at an exposure distance of 2.63 m from the center of the Hg bulb ring. The length of exposure was

controlled based upon the cumulative dosage recorded via the LEM system dosimeters placed next to the test coupons and targeted for exposures of 60, 100, and 140 mJ cm^{-2}. Coupons were exposed to an average intensity calculated to be 0.23-0.24 mW cm^{-2}. Due to the different intensities of the UV sources, the devices were set at different distances from test coupons to achieve similar dosages in an attempt to directly compare the killing efficacy of a broad spectrum light source to a 254 nm source.

For testing, the Xe or Hg rolling units were positioned in the corner of a triangular area and non-reflective folding panels were set up to prevent UV light exposure to personnel outside of the decontamination area. Magnets were glued to the underside of test coupons prior to inoculation of virus and a black, non-reflective, metal sheet rack was utilized as a support for the test coupons. The rack was bent into a curved shape in an attempt to maintain a constant UV exposure distance to all coupons. Testing of these two devices required transport of coupons to the testing site, and coupons were transported in 50 ml conical tubes at room temperature. Negative control coupons as well as additional shipping controls (inoculated and transported, but not exposed to UV light) were also included. Conditions in the testing room were not aseptic but care was taken to avoid contamination at each step and coupons were only transferred to and from the metal rack using sterile forceps. After UV exposure, samples were transferred to new sterile conical tubes and transported back to the microbiology lab for virus extraction and quantification.

Specific testing conditions differed slightly between the two rolling units. For testing the Xenex Lightstrike, the metal stand holding virus-inoculated test coupons was placed such that the coupon height was between 1.09 and 1.55 m above the ground (approximately parallel to the height of the pulsed Xe bulb) and the distance between the coupons and the UV light source was 1.72-1.78 m. Based on preliminary dosage readings, the Xenex Lightstrike did not need a 30-min warm up time. Two time points of 5 and 20 min were tested. Room conditions were measured at 23.3±1°C and 74% RH for the first exposure and 25.1±1°C and 22% RH for the second exposure. As the tests occurred in succession approximately 30 min apart, the shift in environmental conditions with the rise in temperature and drop in humidity is speculated to be driven by Xe unit itself. Additionally, the smell of ozone was detected in the air following the completion of each test.

For testing the LEM, the metal stand holding virus-inoculated test coupons was placed such that the coupon height was approximately 1.2 m above the ground (parallel to center of the Hg bulbs) and the distance between the center of the ring of UV bulbs to the center of the metal arc with coupons was approximately 2.62 m. The distance between the test coupons and the nearest UV bulb was 2.43m. Testing for this device included three independent exposures of 60, 100 and 140 mJ cm^{-2} which took 4 min 22 s, 7 min 2 s, and 9 min 33 s, respectively. The exposure conditions were 26±1°C, 38% RH. Ozone level in the room was measured at 0.08 ppm for the LEM, compared to 0.26 ppm for the Xenex Lightstrike (0.1 ppm is the 8-h Occupational Safety and Health Assessment (OSHA) limit).

Prototype Medium Conveyer

The prototype medium conveyer featured a chamber measuring 2.03 m long x 0.78 m wide x 0.69 m tall that was lined on all interior surfaces with UV-C emitting (254 nm) Hg bulbs,

including below the powered rollers (**Figure 4**). Testing of this device required transport of coupons to the testing site, and coupons were transported in 50 ml conical tubes at room temperature. Negative control coupons as well as additional shipping controls (inoculated and transported, but not exposed to UV light) were also included.

Two rounds of testing were performed with the conveyer device, with slight differences in experimental setup and UV dosages. For both rounds, dosimeters were first used in trial-and-error runs to determine the required run-through time to reach the target UV exposures. The dosimeters used were Roithner LaserTechnick GmbH GIVA-S12SD dosimeters from Vienna, Austria, with dimensions of 4.3-cm x 3.5-cm x 1.8-cm. In the first round of experiments, three dosimeters were horizontally taped to a 2% polyethylene board (46.7-cm x 28.6-cm x 2.54-cm) and were sent through the conveyor to get dosage readings based on exposure time (**Figure 4**). After target exposure times were determined, coupons were placed inside sterile Petri dishes and set on the same polyethylene support board before exposure in the conveyer. The first round of testing included exposures of 60 mJ cm^{-2} (22 s), 100 mJ cm^{-2} (32 s), and 140 mJ cm^{-2} (44 s). Conditions within the conveyer for this round were 27.7 °C, 63.2% RH, 0.09 ppm ozone.

In the second round of testing, the initial runs were again dosimeter-only to determine exposure times to reach the targeted UV dosages. The same dosimeters were used, but this time they were placed on a ceramic tile (~45.7-cm x 45.7-cm). During testing, coupons were placed directly on the ceramic tile support to prevent the sides of the Petri dishes from blocking any UV light from reaching the coupons. Test conditions were 17.3±1°C and 20.1% RH. Ozone reading was not captured since the ozone reader was unavailable.

Figure 4. Dosimeters traveling down conveyor to determine exposure times for target UV dosages.

Prototype Big Box UV Chamber for Pallets

A prototype Big Box UV Sterilizer, a proprietary UV-C decontamination device, was acquired for virus inactivation testing. The outside dimensions were 2.74-m x 2.24-m x 2.4-m with an interior large enough to accommodate a recommended maximum load with dimensions

of 1.21-m wide x 1.21-m long x 1.52-m tall. Max interior load was 1,134 kg. The interior was lined on five surfaces with a total of 320 T8 Hg bulbs, each measuring 0.9 m long and emitting 254 nm UV-C light. A double-stacked pallet mock-up of dimensions 1.02-m x 1.1.22-m x 1.64-m was placed within the UV chamber (**Figure 5**), centered from left to right and positioned up against the rear backstop on the base of the chamber.

During testing, coupons were placed in Petri dishes on top of the pallet in five separate locations, with lids removed prior to exposure. The UV chamber doors were closed, and the chamber was operated via a pre-programmed cycle set to run for 2 min followed by a 30 s exhaust. After UV exposure, the coupons were recovered and the surviving virus was extracted and quantified. There was a single combined 2 min exposure test run for all coupons except for ABS plastic coupons, which was tested for 2 min on a separate test day. Room temperature extraction control samples were transported to and from the test location along with test coupons. Peak ozone generated was 0.36 ppm which is purged prior to opening the doors.

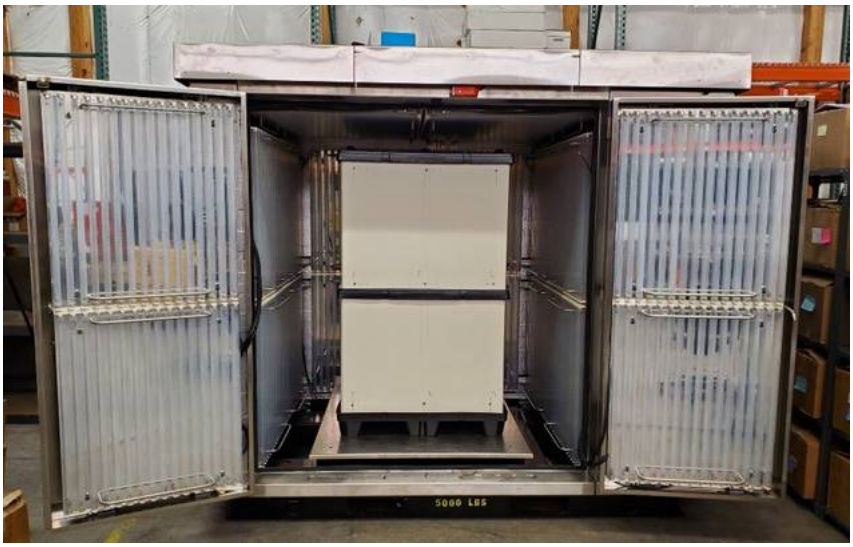

Figure 5. Prototype Big Box UV-C Chamber with a double stacked pallet.

Prototype Fixed UV Devices for Room Decontamination

Three prototype devices were also tested that were intended to be installed on the ceiling or wall to provide viral decontamination of the air. These devices followed the same general concept but differed slightly in design and were tested in iterations that featured different UV light sources (Hg and KrCl bulbs). Test setup for these devices was largely similar to the previous devices, with each test being carried out for five coupons, each inoculated from one of five independent viral preparations. Sterile control and extraction control coupons were also included. However, only one coupon material was tested for each device. Because the purpose of

these devices is air decontamination, the specific test material employed here was not particularly important so long as the material was non-porous with high extraction efficiency and the materials provided no additional decontamination properties. SS304 was initially used for testing, and was later replaced by quartz glass in one case as it allows greater UV transmittance to maximize the surface area that would be exposed to UV light, similar to the way air particles would be exposed at all angles to direct or reflected UV-C light. Tests were carried out for 5, 10, and 15 s for each device, though the distance from the UV source differed for each device as described below. For all experiments, the devices were powered on for at least 30 min prior to testing to mitigate any start-up fluctuations in UV output.

Prototype Device A (Hg bulb and KrCl bulb iterations)

Prototype device A featured an internal UV light source within an enclosed chamber. Fans controlled flow into the chamber where air was exposed to UV-C radiation and then exhausted through vents opposite from the fans. The first prototype contained two Philips TUV 15W/G15 T8 mercury bulbs emitting 254 nm UV-C light. Three fans were mounted in the device to provide airflow at 3,030 l min^{-1} total through an effective inner volume of 24.64 l. This leads to a residence time of 0.49 s that air will be exposed to UV radiation within the upper chamber. Exposures were at 5-cm, 10-cm, and 15-cm from the UV source.

The second iteration of device A replaced the dual Hg bulb with a single, custom KrCl excimer bulb from Far-UV Sterilay that emitted 222 nm UV-C, with the goal of developing a device with good decontamination efficacy that also posed less of a hazard to personnel exposed to the light source. The modified device A also included Teflon reflective surfaces to resist dirt build-up and provide reflectance of the UV-C light. High purity non-crystalline-fused silica glass plates, also called quartz glass, were added to channel airflow parallel to the UV-C source and increase the total contact time between contaminated air and the UV-C light. This increased the total UV dosage applied to air in the unit, thereby providing greater efficacy. The modified prototype device featured three fans providing 1,700 l min^{-1} of airflow each into the unit. One fan is always operated with the UV-C power switch. Two additional power switches are present for each additional fan, therefore, the device can operate at 1,700, 3,400, and 5,100 l min^{-1} airflow. The effective interior volume was 24.33 l.

The efficacy of the UV light source within the modified device A (KrCl bulb) was tested with the lid attached. Inoculated quartz glass test coupons were placed individually into a tray and slid inside the unit through slots cut in the frame. Slots were cut at set distances of 4, 10, and 20 cm from the center of the UV bulb. These distances were aligned to prominent design features in the box. The 4-cm test distance (4-cm from the center of the bulb or 2-cm from the edge of the bulb) aligned to an average distance from the bulb in the middle or second air flow channel. The 10-cm distance aligned to the outer channels just behind the quartz glass, and the 20-cm distance also aligned to the outer channels behind the glass at the furthest distance within the device where air would be exposed to UV-C.

Prototype Device B (Hg bulb and KrCl bulb iterations)

Prototype device B featured a single UV-C source in an open-ended unit. Fans directed airflow into the underside of the unit, and air then exited the frame under and past the UV-C

source and then out into the surrounding room air. As with device A, two iterations of the design were tested. The first iteration contained one Philips TUV PL-L 36W/4P Hg bulb. Device B was designed to be mounted to a wall and featured one fan to draw air upwards from underneath the device and exhaust out the top and upper sides. It required a mounting height of 2.15 m in order to ensure that no humans or pets are exposed to the UV-C light coming out the sides of the device. Test exposures for this device were conducted at 5-cm, 10-cm, and 15-cm from the UV source for 5, 10, and 15 s each. Coupons were placed in plastic Petri dishes with lids removed for exposures.

The second version of device B contained one KrCl excimer bulb emitting 222 nm UV-C light, the same bulb as in the second iteration of device A. With replacement of the 254 nm Hg bulb with 222 nm UV emission, it no longer had the strict requirement of a 2.15 m mounting distance, according to the prototype developer. However, 222-nm UV light exposure were still a concern for Navy personnel. Device B contained limited Teflon as a reflective surface placed near the bulb to direct and concentrate light outward. Unlike device A, device B does not feature a closed compartment where reflectivity with the Teflon can occur (substantially removing that potential for an increase in applied dosage). The device featured a recessed UV compartment between 10-15 cm deep with cross sectional area 38.7-cm x 11.4-cm. The compartment was angled upward at approximately 45° from vertical to exhaust air and provide continuous UV exposure of ambient air. The average measured airflow at the compartment outlet was 2,237 l min^{-1}. Test exposures for this device were conducted at 5, 15, and 30.5, 61 and 122 cm from the UV source for 5, 10, and 15 s each. Coupons were placed in plastic Petri dishes with lids removed for exposures.

Prototype Device C (Hg bulb type only)

Prototype device C followed a similar concept to device B, with a slightly different configuration and form factor. It was designed to be mounted to a wall and featured one Philips TUV 36W/G36 T8 Hg bulb and two internal fans, with the fans placed to draw air upwards through the unit to exhaust out the top and upper sides. Like device B, it requires a mounting height of 2.15 m in order to ensure that no humans or pets are exposed to the UV-C light coming out the upper sides of the device. Test exposures for this device were conducted at 5, 10 and 15 cm from the UV source for 5, 10, and 15 s each. Coupons were placed in plastic Petri dishes with lids removed for exposures.

Φ6 Extraction from Coupons and Plating

An overlay procedure for Φ6 was previously described (Buhr et al. 2020). For Φ6 extraction from materials (coupons), 5 ml of 10mM HEPES + 10% sucrose pH7 were added to each conical tube with a virus-inoculated coupon and vortexed for 2 min. After vortexing, 5 ml of HB10Y log-phase culture (confirmed with real-time Coulter Multisizer analysis) were added and allowed to infect at RT for 15 min, followed by 2 min of vortexing. Each sample was serially diluted, from -2 to -6, in 900 µl of 10 mM HEPES + 10% sucrose pH7. For each Φ6 dilution, from -1 to -6, 200 µl were transferred into individual tubes containing 200 µl log-phase HB10Y. Then 200 µl of those Φ6/HB10Y mixtures were added to individual TSB overlay tubes, poured onto individual TSA plates and allowed to solidify for ≥30 min. Additionally, 1,000 µl was transferred from the 50 ml sample conical tube directly to a TSB overlay tube, and the remaining

558 8.3 ml was poured onto two TSA plates, and also allowed to solidify for ≥30 min. Solidified
559 plates were then inverted, incubated for 20+/-2 h at 26°C and quantified. Plates were incubated
560 an additional 24 h, RT and quantified a final time.

561 Quantitation and calculations of survival were performed as previously described (Buhr
562 et al. 2020). An important difference between virus and prior spore quantitation is that virus and
563 spore inoculum dried on to coupons was stable. However, titers of virus controls stored in
564 solution were unstable and highly variable. Therefore, virus inoculation titers was defined as
565 100% extraction, or maximum recoverable virus, and used to calculate extraction efficiency for
566 each material. This is a key difference compared to spore quantitation because spores are stable
567 in non-nutrient aqueous solution at temperatures up to at least 65°C (Buhr et al. 2012).

RESULTS

568 To increase confidence in decontamination results and to conservatively estimate
569 decontamination requirements for enveloped virus in its native state, enveloped virus test
570 coupons were prepared to be protected similar to a natural virus without interfering with the
571 virus assay. Respiratory illnesses are typically caused by particles within the 0.5-6 μm size range
572 since particles of these sizes aerosolize well and effectively adhere within the lungs (e.g. Hofer et
573 al. 2021). A typical infectious dried particle of this size usually only contains 0-10 live virions,
574 while the remainder of the particle (>99.9%) is primarily composed of salt, mucin glycoprotein
575 (in human airway mucus, 75-90% carbohydrate), and a minor amount of surfactants (Williams et
576 al. 2006; Vejerano and Marr 2018, Hadi et al., 2020, Stadnytskyi et al. 2020). Thus, Φ6 virus
577 was unpurified to maintain natural stabilization with host cell debris, and was diluted in a 10%
578 sucrose solution to mimic the presence of carbohydrates in mucus without inhibiting the
579 decontamination assay (Brakke 1951, Malenovska 2014, Buhr et al. 2020, Hadi et al. 2020,
580 Stadnytskyi et al. 2020). In addition, enveloped virus was dried on coupons prior to testing since
581 SARS-CoV-2 respiratory particles evaporate within seconds to generate dry particles, and drying
582 on fomites is also historically documented as a route of infection for enveloped virus (Fenn 2001,
583 Malenovska 2014, Hadi et al. 2020, Stadnytskyi et al. 2020).

584 Enveloped virus stability had been confirmed previously: purified virus was unstable, but
585 unpurified virus was stable and could be stored dried onto coupons for at least 2 weeks prior to
586 extraction (Buhr et al 2020). Furthermore, there was no Φ6 inactivation after unpurified virus
587 was dried onto different surfaces for at least 24 h, RT followed by a 10 d exposure to 26.7°C at
588 80% RH, and only 2.4 $\log_{10}$ inactivation was seen after treatment at 70°C, 5% RH for 24 h (Buhr
589 et al 2020). More work will be needed to confirm that Φ6 and SARS-CoV-2 are stabilized
590 similarly in the presence of carbohydrates and mucus, and after drying, but the first challenge is
591 to generate sufficient SARS-CoV-2 virus to match the titers (and statistical confidence) of the Φ6
592 tests. This goal has not yet been met. In addition, neither SARS-CoV-2 nor BSL-2 virus field
593 testing is likely to happen with regularity.
594
595 The original quantitative objective was to show enveloped virus inactivation of ≥7 $\log_{10}$
596 out of a ≥8 $\log_{10}$ challenge. This challenge level was set because measurements with high
597 concentrations of microbes greatly increase the confidence in inactivation and mitigate the risk

of incomplete decontamination (Hamilton et al 2013). Furthermore, an individual highly infected with SARS-CoV-2 can emit >8 $\log_{10}$ virus particles in a 24 h period based on published data, and coronavirus nasal swabs showed >8 $\log_{10}$ virus per swab as calculated using a PCR assay (Leung et al. 2020; Stadnytskyi et al. 2020). High challenge levels also increase confidence since exposure limits (infectious dosages) are not well defined for many viruses such as SARS-CoV and SARS-CoV-2. UV light does not fall under the United States Environmental Protection Agency (EPA) jurisdiction for disinfection claims since it is not classified as a chemical disinfectant. However, for this study, the inactivation goal was reduced from 7 $\log_{10}$ to 3 $\log_{10}$ inactivation during the COVID-19 pandemic to match the EPA N-list for decontaminants. This was helpful because inactivation numbers for sanitation, disinfection and sterilization could be used for technical assessments (Rutala et al. 1996). The ≥8 $\log_{10}$ challenge was maintained to meet confidence requirements for end users. This also met the goal of previous work where a ≥7 $\log_{10}$ virus challenge was a threshold and ≥8 $\log_{10}$ virus challenge was an objective (Buhr et al. 2014).

UV Handheld Devices

Two commercial handheld UV devices, the GermAway 18W and 35W handheld sanitizers, and two prototype handheld UV devices, a 272 nm LED prototype and a 222 nm prototype, were tested. The dosage and virus inactivation results are summarized in **Tables 1** ($\log_{10}$ reduction) and **2** ($\log_{10}$ survival). Dosages and virus inactivation were measured at a 5 cm distance, which was considered a reasonable, practical distance for a handheld device used to scan over surfaces. The keyboard keys were slightly taller and closer to the light source. Thus, the dosage on the keys was slightly greater than the other materials but no dosage calculations were made specifically for those keys.

To evaluate the efficacy of the devices, a minimum of 3-$\log_{10}$ inactivation was targeted, which is equivalent to a 99.9% reduction and corresponds to the current EPA requirements for chemical disinfection. A 10 s exposure with the GermAway 18W unit failed to meet the ≥3 $\log_{10}$ inactivation threshold for all tested materials. A 20 s exposure successfully achieved a greater than 3 $\log_{10}$ inactivation out of an 8.2 $\log_{10}$ virus challenge on SS304, NTC, keyboard keys, and polyurethane but failed to meet the 3 $\log_{10}$ inactivation threshold on cardboard.

The GermAwayUV 35W handheld sanitizer failed to meet the ≥3 $\log_{10}$ inactivation threshold out of an 8 $\log_{10}$ PFU virus challenge on all five materials for all three exposure durations, achieving less than 2 $\log_{10}$ PFU inactivation. The GermAwayUV 35W handheld sanitizer delivered lower dosage than the 18W handheld despite nearly double the power. Hence there was no correlation between power and dosage/efficacy, and the importance of measuring every device was apparent.

The 272 nm LED prototype successfully achieved a ≥3 $\log_{10}$ PFU inactivation out of an 8.5 $\log_{10}$ PFU virus challenge for SS304 at 2, 5, and 10 s, for ABS at 5 and 10 s, and for NTC and polyurethane at 10 s. The hardest, smoothest material was SS304 and it showed the greatest $\log_{10}$ reduction at all 3 time points. Cardboard showed the lowest inactivation rate with no treatments providing ≥3 $\log_{10}$ PFU inactivation. Overall, the 272nm LED prototype showed significantly greater virus inactivation compared to the 18W and 35W handheld commercial devices.

The 222nm Excimer UV prototype failed to achieve a >3 log_{10} inactivation out of an 8.5 log_{10} virus challenge for all 5 materials tested, making it the least effective of the four handheld devices tested. Further testing with longer exposure times might produce results passing the ≥3 log_{10} inactivation threshold. From a practical standpoint this data showed that this 222 nm prototype had poor efficacy and very limited utility. Since this was a prototype, iterative improvements can be made to improve performance of this device.

Room Decontamination Devices

Results for a mounted prototype containing a pulsed Xe bulb are shown in **Tables 1** (log_{10} reduction) and **2** (log_{10} survival). This device emitted broad-spectrum light in pulses occurring every 6 s, with the duration of each pulse measured at 0.489 s, and the majority of the dosage applied over the first few milliseconds of that time. Because of the broad spectrum nature, the UV dosage could not be confidently measured. This device demonstrated measurable efficacy at 0.5 m for 60 min and the results were best on non-porous materials. Efficacy was very limited at 1 and 2 m and shorter exposure times, particularly on porous cardboard, followed by semi-porous NTC. As usual, the best efficacy was on the smooth surfaces; plastic and SS304.

Results for the Xenex Lightstrike unit with pulsed Xe UV bulb are shown in **Tables 1** and **2**. The Lightstrike emitted pulses at a rate of 67 per s. Test 1 for 5 min occurred at environmental conditions of 23.3±1°C and 74% RH. Test 2 for 20 min occurred at 25.1±1°C and 22% RH. The 2 tests occurred in succession approximately 30 min apart, and the smell of ozone was detected in the air following the completion of each test. Additionally, the Xenex did not require a warmup time in contrast to devices with Hg bulbs. The Xenex Lightstrike failed to achieve a ≥3 log_{10} inactivation out of an 8.4 log_{10} PFU virus challenge for all 5 materials tested.

Results for the LEM with Hg bulbs are shown in **Tables 1** and **2**. The LEM successfully achieved a ≥3 log_{10} PFU inactivation out of an 8.4 log_{10} PFU virus challenge for SS304 at all three dosages, for polyurethane at the higher two exposures, and for NTC and keyboard keys at the highest dosage only. It failed to meet the ≥3 log_{10} PFU inactivation threshold for cardboard at all three exposure levels.

Prototype Medium Conveyer

Two rounds of testing were carried out for the prototype medium conveyer with Hg bulbs, with each round varying in dosages tested and in the method of exposing the test coupons (see Methods section for this device). The dosages over time were not perfectly linear. The dosage variability over time might have been variability in dosimeter readings and/or variability in Hg bulb dosages after warmup. Test results are shown in **Tables 1** and **2**. During round 1 testing at 60 mJ cm^{-2} (20 s), 100 mJ cm^{-2} (32 s) and 140 mJ cm^{-2} (44 s), the conveyer successfully achieved a ≥3 log_{10} PFU inactivation out of an 8.2 log_{10} PFU virus challenge for all three exposure times on SS304, NTC, ABS plastic, and polyurethane, with slightly higher inactivation results for ABS plastic and polyurethane at the higher two treatments. It failed to meet the ≥3 log_{10} PFU inactivation threshold on cardboard for all three exposure times.

For round 2 of testing, the dosages measured during testing were 13.7 mJ cm^{-2} (8s), 23.8 mJ cm^{-2} (16s), 40.0 mJ cm^{-2} (24s), and 56.2 mJ cm^{-2} (32s). Regardless of dosage variability, the

conveyer successfully achieved a ≥3 log_{10} inactivation out of an 8.4 log_{10} virus challenge for SS304 at 24 and 32 s, for NTC at 32 s, and for ABS plastic at 32 s time points. For all other materials and round 2 exposure times, it failed to reach the ≥3 log_{10} PFU threshold inactivation.

Figure 6 plots the log_{10} reduction from the conveyer against dosage on the different materials. The conveyor produced UV dose-dependent inactivation at lower dosages (13.7-56.2 mJ cm^{-2}), but inactivation leveled off across all surfaces tested at higher dosages (60-140 mJ cm^{-2}). The size of the shielded virus population was dependent on material porosity since the highest level of inactivation was observed on non-porous SS304, followed by polyurethane, ABS plastic, NTC, and then porous cardboard. In addition, an additional sub-population of virus protected by debris was shielded from exposure to radiation because of the presence of host cell debris as indicated by a flattening of the kill rate across all the materials including smooth SS304. That sub-population of debris-complexed virus manifest may manifest higher resistance to the damaging effects of the UV radiation because of both shielding and drying; it is widely known that UV damage produces covalent bonds in nucleic acid and biochemical reactions involving bond formation typically require a solvent like water.

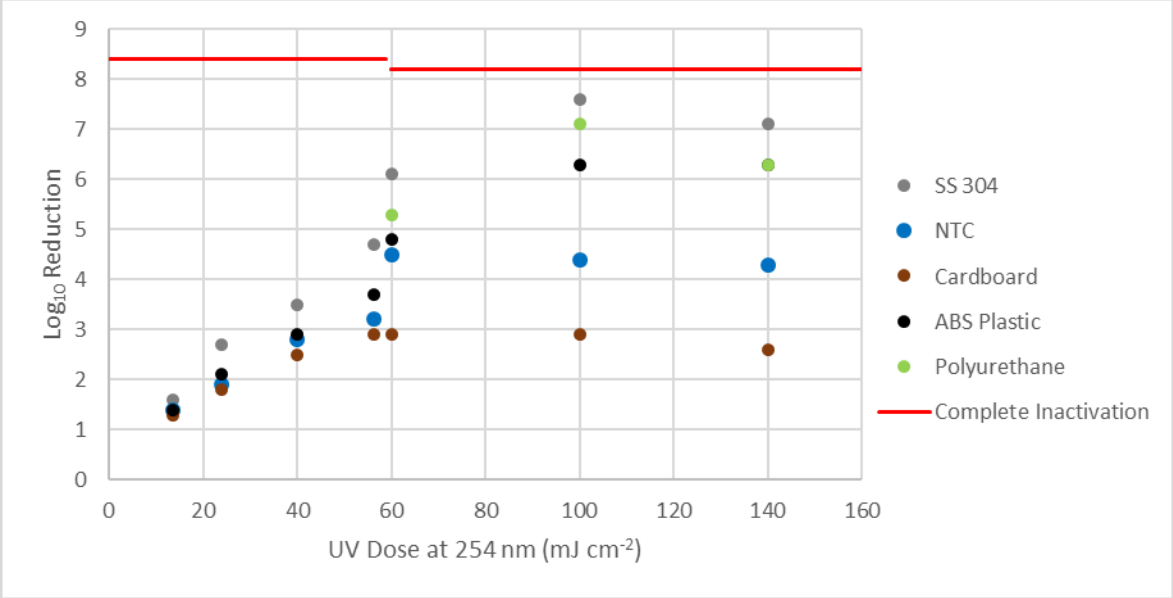

Figure 6. Prototype Medium Conveyor log_{10} reduction.

Prototype Big Box UV Chamber

Results for the prototype Big Box UV sterilizer are shown in summary **Tables 1** and **2**. A large double-stacked pallet mock-up was set inside the Big Box UV sterilizer. Coupons were then set on top of the plastic and cardboard mock-up for UV exposure, and the distance from virus-inoculated coupon to the nearest Hg bulbs on the chamber ceiling was 16.5 cm. The dosages varied significantly at different locations in the box resulting in a dosage range of 377-

729 mJ cm^{-2} for the test materials. Virus inactivation test results after UV treatment of 8.4 log_{10} PFU of enveloped virus deposited per coupon (8.2 log_{10} PFU for ABS plastic) showed a ≥5 log_{10} PFU inactivation for SS304, polyurethane, and ABS plastic and a ≥3 log_{10} PFU inactivation for NTC and cardboard. As for all other devices, the hardest, smoothest material (SS304) was most effectively treated while the most porous material (cardboard) was hardest to decontaminate.

Overall, the prototype Big Box chamber showed higher virus inactivation compared to almost all other devices, corresponding to the significantly higher UV dosage achieved with the large number of Hg bulbs in the chamber. The data highlights the overall limitations of UV technology to provide complete virus inactivation since virus sterilization was not achieved despite a large, powerful system featuring a total of 320 Philips T8 Hg bulbs.

Prototype Fixed UV Devices for Air and/or Surface Decontamination

Devices intended for air decontamination represent a challenge because methods to mimic actual respiratory enveloped virus have yet to be developed. While there are nebulization protocols for wet purified virus, these methods have little practical relevance for field testing of environmentally relevant SARS-CoV-2 virus where the virus is protected by mucus (the surface of which primarily consists of carbohydrate), the infectious particles only consist of ≤0.13% virus, and the infectious 4 um particles are dry, not wet (Hadi et al. 2020; Stadnytskyi et al. 2020). For the purposes of this work, the methods for field testing on virus-inoculated surfaces were maintained in order to comparatively screen and assess the effectiveness of the UV bulbs used in the different prototypes, particularly since there was so much variability in dosage and efficacy among different UV sources up to this point. This approach helped with iterative assessments and prototype improvements.

Mounted Prototypes A, B (Hg bulb and KrCl bulb prototypes), and C (Hg bulb type only):

Results for the mounted prototype A, B and C are shown in **Tables 3** (log_{10} reduction) and **4** (log_{10} survival)**.** For the original prototype A with the Hg bulbs, there was minimal log_{10} reduction at different distances and times against virus-inoculated SS304. A modified prototype version with a greatly optimized internal configuration and a KrCl bulb was tested against virus-inoculated quartz glass. Time and cost restrictions prevented a test on virus-inoculated SS304. The modified prototype A unit was determined to require approximately 5 min for the UV-C output to stabilize. The device was verified to emit a peak wavelength of 222 nm with a slight spike at 252 nm likely from the SiO_2 glass casing of the bulb (data not shown). This modified prototype A unit showed a significant improvement over the original prototype. There were too many significant changes between the first and second prototypes to isolate any single variable as the primary reason for the improved efficacy.

For the original prototype B with a Hg bulb, there was minimal log_{10} reduction at different distances and times against virus-inoculated SS304. A modified prototype B with a KrCl bulb emitting 222 nm UV was tested. Test results showed worse efficacy results than the original prototype B. Overall, this device was the least effective of the wall-mounted prototypes, and it was not modified as extensively compared to the modified prototype A. The 222 nm KrCl bulb clearly did not improve efficacy in this prototype.

Prototype C had the least favorable design, and given its low efficacy, it was not pursued for modification.

DISCUSSION

The focus of this research was to establish reference test methods for UV decontamination of enveloped virus, and to both assess and accelerate improvements in UV devices. Φ6 was selected as a BSL-1, enveloped RNA virus test indicator for both lab and field tests. Φ6 has been widely used as an enveloped virus surrogate (de Carvalgo et al. 2017). It bears structural similarity to many other enveloped viruses including coronaviruses, suggesting that the Φ6 structure should be similarly susceptible to general decontaminants. Furthermore, the structural molecules of the virus are produced by host cells with temperature sensitivity at around 40°C, further suggesting that Φ6 should be similarly susceptible to general decontaminants as animal coronaviruses. The capabilities for measuring UV efficacy using both physics-based equipment and live, enveloped virus test indicators allowed standardized test measurements in both lab and field tests to directly compare the different UV devices.

The UV test results here showed that high UV dosages are needed to inactivate enveloped virus protected by environmental debris, and porous materials are difficult to decontaminate, particularly in comparison with purified virus alone. These limitations of UV light are well documented by regulatory agencies and those limitations also apply to SARS-CoV-2 (Anonymous 2021a and 2021b). Nonetheless, UV efficacy was measurable and very high dosages were effective even on relatively porous materials like cardboard. It is unlikely that UV would be useful for highly porous fabrics used to make bags, carpeting and clothing, and those were not tested. In contrast, hot, humid air inactivates dirty microbes with similar kinetics regardless of material porosity (e.g. Buhr et al 2012, 2015, 2016, 2020). This is a hallmark difference between highly penetrative decontaminants and a surface decontaminant like UV.

The prototype medium conveyer generated the highest virus inactivation per dosage. Inoculated coupons were exposed to UV-C light on three sides since the coupons were set on a flat surface during exposure in the conveyer. The big UV box also generated high levels of virus inactivation, but the medium conveyer was highest efficacy dose^{-1}. In contrast the handheld devices, pulsed Xenon devices, LEM, and the original prototypes A, B, and C, and modified prototype B were all evaluated with a UV source emitted from predominantly one direction with slightly varying angles of exposure. The increased angles of exposure in the conveyer and big box likely improved UV-C penetration. Hence, the unique geometry, design and electronics of each device impacted the effectiveness above and beyond the wavelength and dosage.

Anti-viral efficacy among the different UV devices ranged from no decontamination up to nearly achieving enveloped virus sterilization. Enormous variability in dosage and efficacy was measured within and among the different devices. This variability strongly indicated that all UV devices need to be measured for both UV dosage and for anti-viral efficacy before purchasing and using large numbers of these devices. The efficacy of a pulsed Xe bulb was measurable at close distances, but significantly lower than Hg bulbs. However, pulsed Xe devices do have some practical advantages such as requiring minimal warm up time and no Hg

toxicity. LEDs are also far more practical than Hg bulbs because LEDs have the lowest hazard, lowest variability in UV output, and the 272 nm LED showed highest efficacy. However, the availability of UV LEDs has been limited, and UV dosages can also be limiting depending on the manufacturer, model, the electronics and overall design of any given device. Longer wavelength UV (272 nm) showed the best efficacy in handheld devices and 272 nm is more penetrating than short wavelengths. However, 222 nm KrCl lights showed measurable efficacy in conjunction with proprietary prototype advancements.

Finally, decontamination with UV comes with tradeoffs that affect the decision of the end user. The time of exposure needed to generate efficacy needs to be assessed by end users because long exposure times will limit the utility of UV, especially for handheld and air decontamination devices. Another tradeoff to be assessed by end users is the need for cleaning/maintenance of UV devices to remove dirt/debris that accumulates on the light sources, and/or change light sources. Devices and methods to monitor UV dosage over time are needed to assist in maintenance, a particularly important subject that is rarely addressed. Additional tradeoffs are ozone generation, which can be toxic, and operation times; Hg bulbs in particular require warmup times in order to reach a steady-state. In general, Hg bulbs generate a maximum dosage immediately, and then the dosages were stabilized at a lower level after a warm up period. The Hg devices would have performed better had only this initial dose been tested, but that data would not translate to practical application. Lastly, the end user needs an understanding of the organism(s) to be killed, how it is stabilized in the environment, and the impact of test methods on results, as these factors will impact confidence in any application. Assessment of these tradeoffs will facilitate practical application of UV decontamination. As test standards and UV sources improve, UV will become a more viable option for some decontamination applications. In retrospect, the objective of this work was to catalyze those improvements.

ACKNOWLEDGEMENTS

This work was supported through funding and program support provided by Naval Sea Systems Command, Defense Innovation Unit, Naval Advanced Medical Devices, and the Defense Threat Reduction Agency (DTRA), Hazard Mitigation Capability Area (BA2 and 3 funds, Project Number CB10141). We thank Rich Wiersteiner, Jon Cofield, Heather Ichord, Janet Weir, Glenn Lawson, Chuck Bass, James Noah, John Aaron Miller and Joe Schumer for support. We thank Jason A. Fallen for outstanding technical support, Kira Baugh and Julie Caruana for assistance with editing the paper. This manuscript was approved for public release on 1/27/2022 as #6156; NSWCDD PN-22-00021, and will be released as a pre-print at bioRxiv (Buhr et al.).

COMPETING INTERESTS

None reported

REFERENCES

829 Anonymous - ASTM. (2020). Guidance on SARS-CoV-2 Surrogate Selection.
830 https://www.astm.org/COVID-19/ [Accessed on September 15, 2021].

831 Anonymous – United States Food and Drug Administration. (2021a). UV Lights and Lamps:
832 Ultraviolet-C Radiation, Disinfection, and Coronavirus. https://www.fda.gov/medical-
833 devices/coronavirus-covid-19-and-medical-devices/uv-lights-and-lamps-ultraviolet-c-radiation-
834 disinfection-and-coronavirus. [Accessed on September 15, 2021].

835 Anonymous – Environmental Protection Agency. (2021b). Disinfecting Surfaces with UV Light
836 to Reduce Exposure to SARS-CoV-2. https://www.epa.gov/covid19-research/disinfecting-
837 surfaces-uv-light-reduce-exposure-sars-cov-2. [Accessed on September 15, 2021].

838 Bibby, K., Casson, L.W., Stachler, E. and Haas, C.N. (2015). Ebola Virus Persistence in the
839 Environment: State of the Knowledge and Research Needs. *Environ. Sci. Technol. Lett.* 2, 2−6.
840 https://doi.org/10.1021/ez5003715

841 Brakke, M. K. (1951). Density gradient centrifugation: A new separation technique. *J. Am.*
842 *Chem. Soc.* 73:1847-1848.

843 Buhr, T. L., Young, A. A., Minter, Z.A., Wells, C.M. (2012). Test method development to
844 evaluate hot, humid air decontamination of materials contaminated with *Bacillus anthracis*
845 ΔSterne and *B. thuringiensis* Al Hakam spores. *J Appl Microbiol* **113**, 1037–1051.
846 https://doi.org/10.1111/j.1365-2672.2012.05423.x
847
848 Buhr, T., Young, A.A., Johnson, C.A., Minter, Z., Wells, C., (2014). Decontamination of
849 materials contaminated with *Francisella philomiragia* or MS2 bacteriophage using PES-Solid, a
850 solid source of peracetic acid. *J Appl Microbiol* **117,** 397-404. https://doi.org/10.1111/jam.12540
851
852 Buhr, T., Young, A.A., Barnette, H., Minter, Z.A., Kennihan, N., McPherson, D.C., Johnson,
853 C.A., Bohmke, M., DePaola, M. and Page, M. (2015). Test methods and response surface models
854 for hot, humid air decontamination of materials contaminated with dirty spores of *Bacillus*
855 *anthracis* ΔSterne and *B. thuringiensis* Al Hakam. *J. Appl. Microbiol.* 119, 1263-1277.

856 Buhr, T., Young, A., Bensman, M., Minter, Z., Kennihan, N., Johnson, C., Bohmke, M.,
857 Borgers-Klonkowski, E., Osborn, E., Avila, S., Theys, A. and Jackson, P. (2016). Hot, humid air
858 decontamination of a C-130 aircraft contaminated with spores of two acrystalliferous *Bacillus*
859 *thuringiensis* strains, surrogates for *Bacillus anthracis*. *J. Appl. Microbiol*. 120, 1074-1084.
860 https://doi.org/10.1111/jam.13055

861 Buhr T. L., Young A. A., Borgers-Klonkowski E., Kennihan N. L., Barnette H. K., Minter Z. A.,
862 Bohmke M. D., Osborn E. B., Hamilton S. M., Kimani M. B., Hammon M. W., Miller C. T.,
863 Mackie R. S., Innocenti J. M., Bensman M. D., Gutting B. W., Lilly S. D., Hammer E. E., Yates
864 V. L., Luck B. B. (2020). Hot, Humid Air Decontamination of Aircraft Confirmed That High
865 Temperature and High Humidity Are Critical for Inactivation of Infectious, Enveloped

Ribonucleic Acid (RNA) Virus. *Front Bioeng Biotechnol.* Oct 23;8:592621. https://doi.org/10.3389/fbioe.2020.592621

Chan, K. H., Malik Peiris, J. S., Lam, S. Y., Poon, L. L. M. , Yuen, K. Y. and Seto, W. H. (2011). The Effects of Temperature and Relative Humidity on the Viability of the SARS Coronavirus. *Adv Virology*, Article ID 734690, 7 pages. https://doi.org/10.1155/2011/734690

de Carvalgo, N.A., Stachler, E.N., Cimabue, N. and Bibby, K. (2017). Evaluation of Phi6 persistence and suitability as an enveloped virus surrogate. *Environ. Sci. Technol*. 51 (15), 8692–8700. https://doi.org/10.1021/acs.est.7b01296

Fedorenko, A., Grinberg, M., Orevi, T. and Kashtan, N. (2020). Survival of the enveloped bacteriophage Phi6 (a surrogate for SARS-CoV-2) in evaporated saliva microdroplets deposited on glass surfaces. *Scientific Reports* 10:22419. https://doi.org/10.1038/s41598-020-79625-z

Fenn, Elizabeth A. (2001). Pox Americana: The Great Smallpox Epidemic of 1775-82. New York: Hill and Wang.

Gallandat, K. and Lantagne, D. (2017). Selection of a Biosafety Level 1 (BSL-1) surrogate to evaluate surface disinfection efficacy in Ebola outbreaks: Comparison of four bacteriophages. *PLOS ONE*. 12(5). https://doi.org/10.1371/journal.pone.0177943

Greiff D., Blumenthal H., Chiga, M., Pinkerton, H. (1954). The effects on biologic materials of freezing and drying by vacuum sublimation II. Effect on influenza virus. *J Exptl Med* 100(1): 89-101.

Greiff D., Rightel, W. (1966). Freezing and freeze-drying of viruses In: HT Meryman (Eds.). Cryobiology. Academic Press, Inc, New York, USA. pp. 697-728.

Hadi, J., Dunowska, M., Wu, S., and Brightwell, G. (2020). Control Measures for SARS-CoV-2: A Review on Light-Based Inactivation of Single-Stranded RNA Viruses. *Pathogens* 9: 737-767; https://doi.org/10.3390/pathogens9090737

Hamilton, M., Hamilton, G., Goeres, D. and Parker, A. (2013). Guidelines for the statistical analysis of a collaborative study of a laboratory disinfectant product performance test method. *JAOAC International* 96 (5), 1138-1151. https://doi.org/10.5740/jaoacint.12-217

Heßling, M., Hönes, K., Vatter, P., Lingenfelder, C. (2020). Ultraviolet irradiation doses for coronavirus inactivation – review and analysis of coronavirus photoinactivation studies. *GMS Hygiene and Infection Control* 2020, Vol. 15, ISSN 2196-5226 https://dx.doi.org/10.3205%2Fdgkh000343

Hendley, J.O., Wenzel, R.P., and Gwaltney, J.M., Jr. (1973). Transmission of Rhinovirus Colds by Self-Inoculation. *N Engl J Med* 288:1361–1364.

899 Hofer, S., Hofstätter, N., Duschl, A., and Himly, M. (2021). SARS-CoV-2-Laden Respiratory
900 Aerosol Deposition in the Lung Alveolar-Interstitial Region Is a Potential Risk Factor for Severe
901 Disease: A Modeling Study. *J. Pers. Med*. 11, 431. https://doi.org/10.3390/jpm11050431

902 Leung, N.H.L., Chu, D.K.W., Shiu, E.Y.C., Chan, K.-H., McDevitt, J.J., Hau, B.J.P., Yen, H.-L.,
903 Li, Y., Ip, D.K.M., Peiris, J.S.M., Seto, W.H., Leung, G.M., Milton, D.K. and Cowling, B.J.
904 (2020). Respiratory Virus Shedding in Exhaled Breath and Efficacy of Face Masks. *Nature*
905 *Medicine* 26, 676-680. https://doi.org/10.1038/s41591-020-0843-2

906 Malenovska, H. (2014). The influence of stabilizers and rates of freezing on preserving of
907 structurally different animal viruses during lyophilization and subsequent storage. *J Appl*
908 *Microbiol* 117, 1810—1819. https://doi.org/10.1111/jam.12654

909 McDonnell, G., and Burke, P. (2011). Disinfection: is it time to reconsider Spaulding? *J. Hosp.*
910 *Inf.* 78, 163–170. doi: 10.1016/j.jhin.2011.05.002 https://doi.org/10.1016/j.jhin.2011.05.002

911 Mindich, L. (2004). Packaging, replication and recombination of the segmented genomes of
912 bacteriophage Φ6 and its relatives. *Virus Research*. 101, 83–92.
913 https://doi.org/10.1016/j.viruses.2003.12.008

914 Raiszadeh, M., and Adeli, B. (2020). A Critical Review on Ultraviolet Disinfection Systems
915 against COVID-19 Outbreak: Applicability, Validation, and Safety Considerations. *ACS*
916 *Photonics.* 7 (11):2941-2951. https://doi.org/10.1021/acsphotonics.0c01245

917 Russell, C. J. (2021). Hemagglutinin Stability and Its Impact on Influenza A Virus Infectivity,
918 Pathogenicity, and Transmissibility in Avians, Mice, Swine, Seals, Ferrets, and Humans. *Viruses*
919 13, 746. https://doi.org/10.3390/v13050746

920 Rutala, W.A. and APIC Committee (1996) APIC Guideline for selection and use of disinfectants.
921 *Am J Infect Cont* 24:313-342. https://doi.org/10.1016/S0196-6553(96)90066-8

922 Stadnytskyi, V., Bax, C. E., Bax, A. and Anfinrud, P. (2020). The airborne lifetime of small
923 speech droplets and their potential importance in SARS-CoV-2 transmission. *Proc Natl Acad Sci*
924 117(2), 11875-11877. https://doi.org/10.1073/pnas.2006874117

925 Tseng, C.C.; Li, C.S. (2005). Inactivation of virus-containing aerosols by ultraviolet germicidal
926 irradiation. *Aerosol Sci. Technol*. 39: 1136–1142.
927 https://dx.doi.org/10.1080%2F15459620701329012

928 Van Etten, J., Lane, L., Gonzalez, C., Partridge, J. and Vidaver, A. (1976). Comparative
929 properties of bacteriophage phi6 and phi6 nucleocapsid. *J. Virol*. 18(2), 652–658.

930 Vejerano, E.P.; Marr, L.C. Physico-chemical characteristics of evaporating respiratory fluid
931 droplets. (2018). *J. R. Soc. Interface* 15. https://doi.org/10.1016/j.jaerosci.2021.105760

Vidaver, A.K., Roski, R.K., and Van Etten, J.L. (1973). Bacteriophage phi6: a lipid-containing virus of Pseudomonas phaseolicola. *J. Virol*. 11(5), 799-805.

Weber, T. P. and Stilianakis, K. I. (2008). Inactivation of influenza A viruses in the environment and modes of transmission: A critical review. *J. Inf.* 57, 361-373. doi: 10.1016/j.jinf.2008.08.013 https://doi.org/10.1016/j.jinf.2008.08.013

Wiggington, K.R., Pecson, B.M., Sigstam, T., Bosshard, F. and Kohn, T. (2012). Virus inactivation mechanisms: impact of disinfectants on virus function and structural integrity. *Environ. Sci. Technol*. 46(21), 12069-12078. https://doi.org/10.1021/es3029473

Williams, O.W.; Sharafkhaneh, A.; Kim, V.; Dickey, B.F.; Evans, C.M. (2006). Airway Mucus From Production to Secretion. *Am. J. Respir. Cell. Mol. Biol*. 34, 527–536. https://doi.org/10.1165/rcmb.2005-0436sf

Table 1. Dosage and efficacy of handheld, room and chamber-type devices showing log_{10} reduction data**.** Handheld and room decontaminating devices were tested by exposing coupons to UV at use-case exposure distances and times. The conveyer prototype was tested via positioning coupons on the rollers in the center of the conveyor, and the big box prototype tested via positioning coupons on top of a double-stacked pallet placed inside the unit. Legend: White = Fail <2 log_{10}; low decontamination; Yellow = Fail ≥2 log_{10}, <3 log_{10}; sanitation, Light Blue = Pass ≥ 3 log_{10}; disinfection, and Dark Blue = Pass ≥ 6 log_{10}; approaching virus sterilization. Dosage is based on the steady state emission, not peak emission. Due to the broad spectrum nature of the pulsed Xe bulb, dosage could not be accurately calculated. N/A – dosage measurements had no meaning because of the broad spectrum light source.

Name	Description	Dosage (mJ cm^{-2})	Exposure Distance	Exposure Time	Efficacy (Log_{10} Reduction after an >8 log_{10} challenge of live Φ6)				
					SS 304	NTC	Cardboard	Keyboard Keys/ABS	Polyurethane
GermAway UV 18W Handheld	2 12.7 cm Hg U-shape bulbs in handheld device 254 nm UV-C MSRP $100	101.2	5 cm	10 s	2.5 ± 0.1	2.0 ± 0.0	1.9 ± 0.0	1.9 ± 0.0	2.0 ± 0.0
		202.4	5 cm	20 s	4.3 ± 0.2	3.1 ± 0.2	2.0 ± 0.1	4.5 ± 0.1	3.3 ± 0.1
GermAway UV 35W Handheld	2 22.5 cm Hg twin tube bulbs in handheld device 254 nm UV-C MSRP $450	13.8	5 cm	2 s	0.3 ± 0.0	0.2 ± 0.0	0.3 ± 0.0	0.3 ± 0.0	0.3 ± 0.0
		34.5	5 cm	5 s	0.9 ± 0.1	0.6 ± 0.0	0.7 ± 0.0	0.8 ± 0.1	0.7 ± 0.0
		69.0	5 cm	10 s	1.4 ± 0.1	1.2 ± 0.1	1.2 ± 0.0	1.3 ± 0.0	1.1 ± 0.1
272 nm Prototype Handheld	8 LED strips divided by angled plastic in handheld device 272 nm UV-C	31.2	5 cm	2 s	3.0 ± 0.3	1.6 ± 0.2	1.6 ± 0.1	1.6 ± 0.2	1.6 ± 0.2
		78.0	5 cm	5 s	5.2 ± 0.1	2.8 ± 0.1	2.5 ± 0.2	3.1 ± 0.2	2.0 ± 0.9
		156	5 cm	10 s	6.2 ± 0.4	3.8 ± 0.2	2.4 ± 0.1	4.9 ± 0.2	4.7 ± 0.5
222 nm Excimer Prototype Handheld	3 UV lights attached to 2.54 cm thick plastic panel in handheld device 222 nm UV-C	5.9	5 cm	2 s	0.6 ± 0.1	0.4 ± 0.2	0.1 ± 0.1	0.3 ± 0.1	0.3 ± 0.1
		14.8	5 cm	5 s	0.9 ± 0.2	0.1 ± 0.1	0.5 ± 0.1	0.5 ± 0.1	0.6 ± 0.2
		29.6	5 cm	10 s	1.1 ± 0.2	0.9 ± 0.1	0.6 ± 0.1	0.9 ± 0.1	1.1 ± 0.1
Mounted Pulsed-Xenon Prototype	Pulsed-Xe bulb in small housing ceiling, wall, or tripod-mounted Broad-spectrum UV-B, UV-C	N/A	0.5 m	15 min	1.4 ± 0.1	1.1 ± 0.1	1.1 ± 0.1	1.5 ± 0.1	N/A
			0.5 m	30 min	2.3 ± 0.1	2.3 ± 0.1	1.6 ± 0.1	2.9 ± 0.1	N/A
			0.5 m	60 min	5.2 ± 0.2	3.2 ± 0.3	2.4 ± 0.2	5.2 ± 0.2	N/A
			1 m	15 min	0.5 ± 0.0	0.4 ± 0.1	0.4 ± 0.1	0.3 ± 0.1	N/A
			1 m	30 min	0.8 ± 0.0	0.7 ± 0.0	0.7 ± 0.1	0.7 ± 0.0	N/A
			1 m	60 min	1.5 ± 0.1	1.3 ± 0.1	1.0 ± 0.0	1.3 ± 0.1	N/A
			2 m	15 min	0.0 ± 0.1	0.1 ± 0.1	0.2 ± 0.0	0.1 ± 0.0	N/A
			2 m	30 min	0.1 ± 0.0	0.0 ± 0.0	0.2 ± 0.0	0.2 ± 0.1	N/A
			2 m	60 min	0.3 ± 0.0	0.2 ± 0.1	0.3 ± 0.0	0.2 ± 0.0	N/A
Xenex Lightstrike	1 pulsed-Xe bulb mounted on rolling cart Broad-spectrum UV-B, UV-C MSRP $125,000	N/A	178 cm	5 min	0.8 ± 0.1	0.4 ± 0.0	0.5 ± 0.0	0.5 ± 0.0	N/A
		N/A	178 cm	20 min	1.7 ± 0.0	1.5 ± 0.1	1.3 ± 0.0	2.2 ± 0.1	NA
Light Emitting Module (LEM)	20 Hg bulbs mounted in a ring on rolling cart 254 nm UV-C MSRP $95,000	60	263 cm	4 min 22 s	3.1 ± 0.3	2.6 ± 0.2	1.6 ± 0.1	2.5 ± 0.2	2.1 ± 0.1
		100	263 cm	7 min 2 s	4.6 ± 0.5	2.7 ± 0.2	2.2 ± 0.1	2.7 ± 0.2	3.1 ± 0.1
		140	263 cm	9 min 33 s	5.3 ± 0.5	3.4 ± 0.1	2.7 ± 0.1	4.0 ± 0.2	3.9 ± 0.1
Medium Conveyer Prototype	Chamber lined on 4sides with Hg bulbs, powered conveyer belt to move items through 254 nm UV-C	60	62 cm	20 s	6.1 ± 0.2	4.5 ± 0.1	2.9 ± 0.3	4.8 ± 0.2	5.3 ± 0.1
		100	62 cm	32 s	7.6 ± 0.3	4.4 ± 0.2	2.9 ± 0.2	6.3 ± 0.2	7.1 ± 0.3
		140	62 cm	44 s	7.1 ± 0.4	4.3 ± 0.5	2.6 ± 0.1	6.3 ± 0.3	6.3 ± 0.3
		13.7	62 cm	8 s	1.6 ± 0.2	1.4 ± 0.1	1.3 ± 0.1	1.4 ± 0.1	N/A
		23.8	62 cm	16 s	2.7 ± 0.2	1.9 ± 0.1	1.8 ± 0.1	2.1 ± 0.1	N/A
		40.0	62 cm	24 s	3.5 ± 0.3	2.8 ± 0.1	2.5 ± 0.1	2.9 ± 0.1	N/A
		56.2	62 cm	32 s	4.7 ± 0.4	3.2 ± 0.2	2.9 ± 0.1	3.7 ± 0.1	N/A
Big Box Prototype	Chamber lined on sides and top with Hg bulbs (total 320) 254 nm UV-C	377-729	17 cm	2 min	5.4 ± 0.2	3.6 ± 0.3	3.1 ± 0.2	5.7 ± 0.1	5.4 ± 0.3

963 **Table 2**. Dosage and efficacy of handheld, room and chamber-type devices showing log_{10}
964 survival data**.** Handheld and room decontaminating devices were tested by exposing coupons to
965 UV at use-case exposure distances and times. The conveyer prototype was tested via positioning
966 coupons on the rollers in the center of the conveyor, and the big box prototype tested via
967 positioning coupons on top of a double-stacked pallet placed inside the unit. Legend: White =
968 Fail <2 log_{10}; low decontamination; Yellow = Fail ≥2 log_{10}, <3 log_{10}; sanitation, Light Blue =
969 Pass ≥ 3 log_{10}; disinfection, and Dark Blue = Pass ≥ 6 log_{10}; approaching virus sterilization.
970 Dosage is based on the steady state emission, not peak emission. Due to the broad spectrum
971 nature of the pulsed Xe bulb, dosage could not be accurately calculated. N/A – dosage
972 measurements had no meaning because of the broad spectrum light source.

Name	Description	Dosage (mJ cm^{-2})	Exposure Distance	Exposure Time	Log_{10} Survival after a >8 log_{10} challenge of live Φ6					
					Control	SS 304	NTC	Cardboard	Keyboard Keys/ABS	Polyurethane
GermAway UV 18W Handheld	2 12.7 cm U-shape Hg bulbs in handheld device 254 nm UV-C MSRP $100	101.2	5 cm	10 s	8.4 +/- 0.1	5.9 ± 0.5	6.4 ± 0.1	6.5 ± 0.1	5.5 ± 1.1	6.4 ± 0.1
		202.4	5 cm	20 s	8.2 +/- 0.0	3.9 ± 0.4	5.0 ± 0.4	6.1 ± 0.3	3.7 ± 0.3	5.1 ± 0.2
GermAway UV 35W Handheld	2 22.5 cm twin tube Hg bulbs in handheld device 254 nm UV-C MSRP $450	13.8	5 cm	2 s	8.2 +/- 0.1	7.8 ± 0.2	7.9 ± 0.1	7.8 ± 0.1	7.8 ± 0.2	7.8 ± 0.1
		34.5	5 cm	5 s		7.2 ± 0.2	7.5 ± 0.1	7.3 ± 0.1	7.3 ± 0.3	7.4 ± 0.1
		69.0	5 cm	10 s		6.6 ± 0.3	6.9 ± 0.2	6.9 ± 0.1	6.8 ± 0.2	7.0 ± 0.2
272 nm Prototype Handheld	8 LED strips divided by angled plastic in handheld device 272 nm UV-C	31.2	5 cm	2 s	8.5 +/- 0.2	5.5 ± 0.6	7.0 ± 0.3	6.9 ± 0.2	6.9 ± 0.3	6.9 ± 0.4
		78.0	5 cm	5 s		3.3 ± 0.0	5.7 ± 0.1	6.0 ± 0.4	5.4 ± 0.3	6.5 ± 1.9
		156	5 cm	10 s		2.3 ± 0.7	4.7 ± 0.3	6.1 ± 0.1	3.6 ± 0.5	3.8 ± 0.9
222 nm Excimer Prototype Handheld	3 lamp modules attached to 2.54 cm thick plastic panel, in handheld device 222 nm UV-C	5.9	5 cm	2 s	8.3 +/- 0.2	7.7 ± 0.2	7.9 ± 0.3	8.2 ± 0.1	8.0 ± 0.1	7.9 ± 0.0
		14.8	5 cm	5 s		7.4 ± 0.3	8.2 ± 0.1	7.8 ± 0.1	7.8 ± 0.2	7.6 ± 0.3
		29.6	5 cm	10 s		7.1 ± 0.4	7.1 ± 0.4	7.6 ± 0.1	7.4 ± 0.2	7.1 ± 0.1
Mounted Pulsed-Xenon Prototype	Pulsed-Xe bulb in small housing ceiling, wall, or tripod-mounted Broad-spectrum UV-B, UV-C	N/A	0.5 m	15 min	8.2 +/- 0.1	6.8 ± 0.2	7.0 ± 0.2	7.1 ± 0.2	6.7 ± 0.1	N/A
			0.5 m	30 min		5.9 ± 0.3	5.8 ± 0.3	6.6 ± 0.1	5.3 ± 0.2	N/A
			0.5 m	60 min		2.9 ± 0.4	5.0 ± 0.8	5.7 ± 0.5	3.0 ± 0.6	N/A
			1 m	15 min		7.7 ± 0.1	7.7 ± 0.2	7.7 ± 0.1	7.8 ± 0.1	N/A
			1 m	30 min		7.4 ± 0.1	7.5 ± 0.0	7.4 ± 0.1	7.4 ± 0.1	N/A
			1 m	60 min		6.7 ± 0.2	6.8 ± 0.2	7.2 ± 0.1	6.8 ± 0.2	N/A
			2 m	15 min		8.2 ± 0.1	8.1 ± 0.1	8.0 ± 0.1	8.1 ± 0.0	N/A
			2 m	30 min		8.1 ± 0.1	8.1 ± 0.1	8.0 ± 0.1	8.0 ± 0.1	N/A
			2 m	60 min		7.9 ± 0.0	7.9 ± 0.1	7.8 ± 0.1	7.9 ± 0.1	N/A
Xenex Lightstrike	1 pulsed-Xe bulb mounted on rolling cart Broad-spectrum UV-B, UV-C MSRP $125,000	N/A	178 cm	5 min	8.4 +/- 0.0	7.6 ± 0.2	8.0 ± 0.1	7.9 ± 0.1	7.8 ± 0.1	N/A
		N/A	178 cm	20 min		6.7 ± 0	6.9 ± 0.3	7.1 ± 0.0	6.2 ± 0.1	N/A
Light Emitting Module (LEM)	20 Hg bulbs mounted in a ring on rolling cart 254 nm UV-C MSRP $95,000	60	263 cm	4 min 22 s	8.4 +/- 0.2	5.3 ± 0.6	5.8 ± 0.5	6.8 ± 0.2	5.9 ± 0.5	6.3 ± 0.1
		100	263 cm	7 min 2 s		3.8 ± 1.1	5.7 ± 0.5	6.2 ± 0.2	5.7 ± 0.4	5.3 ± 0.1
		140	263 cm	9 min 33 s		3.1 ± 1.1	5.0 ± 0.3	5.8 ± 0.2	4.4 ± 0.3	4.6 ± 0.2
Medium Conveyer Prototype	Chamber lined on 4 sides with Hg bulbs, powered conveyer belt to move items through 254 nm UV-C	60	62 cm	20 s	8.2 +/- 0.1	2.1 ± 0.4	3.7 ± 0	5.3 ± 0.6	3.4 ± 0.4	2.9 ± 0.1
		100	62 cm	32 s		0.6 ± 0.6	3.8 ± 0.5	5.3 ± 0.4	2.0 ± 0.4	1.1 ± 0.7
		140	62 cm	44 s		1.1 ± 0.8	3.9 ± 1.1	5.6 ± 0.1	1.9 ± 0.6	0.9 ± 0.5
		13.7	62 cm	8 s	8.4 +/- 0.2	6.8 ± 0.4	7.0 ± 0.1	7.1 ± 0.1	7.0 ± 0.1	N/A
		23.8	62 cm	16 s		5.6 ± 0.4	6.5 ± 0.1	6.5 ± 0.2	6.3 ± 0.1	N/A
		40.0	62 cm	24 s		4.8 ± 0.6	5.5 ± 0.2	5.8 ± 0.3	5.4 ± 0.2	N/A
		56.2	62 cm	32 s		3.7 ± 1.0	5.1 ± 0.4	5.5 ± 0.2	4.7 ± 0.1	N/A
Big Box Prototype	Chamber lined on sides and top with Hg bulbs (total 320) 254 nm UV-C	377-729	17 cm	2 min	8.4 +/- 0.1	3.0 ± 0.4	4.8 ± 0.6	5.3 ± 0.5	2.5 ± 0.3	3.0 ± 0.6
					8.2 +/- 0.1 (ABS plastic only)					

973 **Table 3.** Dosage and efficacy of room-air-irradiating prototypes showing log_{10} reduction data.
974 Prototypes were tested at representative exposure distances but the exposure times were much
975 longer than expected for application in order to provide modeling data. Bio-efficacy testing on
976 the original prototypes A, B, and C evaluated the performance of the UV light source only.
977 Testing on the modified prototypes A and B evaluated the internal improvements to the device.
978 Thus bio-efficacy data presented would be significantly less if realistic, shorter times were tested.
979 Legend: White = Fail <2 log_{10}; low decontamination; Yellow = Fail ≥2 log_{10}, <3 log_{10};
980 sanitation, Light Blue = Pass ≥ 3 log_{10}; disinfection, and Dark Blue = Pass ≥ 6 log_{10}; approaching
981 virus sterilization. Dosage is based on the average power from the bulb area, not the peaks. .
982 Efficacy values indicate log_{10} reduction after a ≥8 log_{10}- challenge of live, dried enveloped virus.

Name	Description	Dosage (mJ cm^{-2})	Exposure Distance (cm)	Exposure Time (s)	Efficacy (Log_{10} Reduction after a >8 log_{10} challenge of live Φ6)	
					SS 304	Quartz Glass
Ceiling-mounted prototype A: Original	2 Hg bulbs within enclosed chamber; fans circulate air through unit 254 nm UV-C	18.6	5	5	0.9 ± 0.1	NA
		37.2		10	1.3 ± 0.1	NA
		55.8		15	1.7 ± 0.1	NA
		12.9	10	5	0.6 ± 0.1	NA
		25.7		10	1.0 ± 0.1	NA
		38.6		15	1.3 ± 0.1	NA
		10.6	15	5	0.5 ± 0.1	NA
		21.1		10	0.8 ± 0.1	NA
		31.7		15	1.1 ± 0.1	NA
Wall-mounted device A: Modified	KrCl/Excimer lamp within enclosed chamber; fans circulate air through unit 222 nm UV-C	15.2	4	5	NA	5.5 ± 0.6
		30.5		10	NA	6.4 ± 0.3
		45.8		15	NA	6.6 ± 0.7
		6.9	10	5	NA	2.2 ± 0.2
		13.7		10	NA	4.6 ± 0.7
		20.6		15	NA	6.7 ± 0.2
		3.4	20	5	NA	1.3 ± 0.1
		6.8		10	NA	2.4 ± 0.3
		10.2		15	NA	4.0 ± 0.6
Wall-mounted prototype B: Original	Hg bulb within open sconce; fans circulate air through unit 254 nm UV-C	29.9	5	5	1.6 ± 0.1	NA
		59.8		10	2.5 ± 0.1	NA
		89.7		15	3.4 ± 0.1	NA
		15.8	10	5	1.1 ± 0.1	NA
		31.6		10	1.7 ± 0.1	NA
		47.4		15	2.3 ± 0.1	NA
		9.9	15	5	0.8 ± 0.1	NA
		19.7		10	1.3 ± 0.2	NA
		29.6		15	1.5 ± 0.1	NA
Wall-mounted prototype B:: Modified	KrCl/Excimer lamp within open sconce; fans circulate air through unit 222 nm UV-C	15.6	5	5	0.5 ± 0.1	NA
		31.2		10	0.9 ± 0.2	NA
		46.8		15	1.2 ± 0.3	NA
		7.5	15	5	0.6 ± 0.2	NA
		15.0		10	0.5 ± 0.3	NA
		22.5		15	0.9 ± 0.1	NA
		2.8	30.5	5	0.1 ± 0.1	NA
		5.6		10	0.2 ± 0.1	NA
		8.4		15	0.2 ± 0.2	NA
		0.2	61	5	0.0 ± 0.2	NA
		0.3		10	0.0 ± 0.2	NA
		0.5		15	0.1 ± 0.1	NA
		0.1	71	5	0.0 ± 0.1	NA
		0.2		10	0.0 ± 0.1	NA
		0.3		15	0.0 ± 0.1	NA
Wall-mounted prototype C	Hg bulb within open sconce; fans circulate air through unit 254 nm UV-C	16.6	5	5	0.9 ± 0.2	NA
		33.2		10	1.6 ± 0.0	NA
		49.8		15	2.2 ± 0.2	NA
		9.1	10	5	0.7 ± 0.1	NA
		18.2		10	0.9 ± 0.1	NA
		27.3		15	1.3 ± 0.1	NA
		6.4	15	5	0.5 ± 0.1	NA
		12.8		10	0.8 ± 0.0	NA
		19.2		15	1.2 ± 0.1	NA

983

Table 4. Dosage and efficacy of room-air-irradiating prototypes showing log_{10} survival data. Prototypes were tested at representative exposure distances but the exposure times were much longer than expected for application in order to provide modeling data. Bio-efficacy testing on the original prototypes A, B, and C evaluated the performance of the UV light source only. Testing on the modified prototypes A and B evaluated the internal improvements to the device. Thus bio-efficacy data presented would be significantly less if realistic, shorter times were tested. Legend: White = Fail <2 log_{10}; low decontamination; Yellow = Fail ≥2 log_{10}, <3 log_{10}; sanitation, Light Blue = Pass ≥ 3 log_{10}; disinfection, and Dark Blue = Pass ≥ 6 log_{10}; approaching virus sterilization. Dosage is based on the average power from the bulb area, not the peaks. Efficacy values indicate log_{10} reduction after a ≥8 log_{10}- challenge of live, dried enveloped virus.

Name	Description	Dosage (mJ cm^{-2})	Exposure Distance (cm)	Exposure Time (s)	Log_{10} Survival after a >8 log_{10} challenge of live Φ6		
					Control	SS 304	Quartz Glass
Ceiling-mounted Prototype A: Original	2 Hg bulbs within enclosed chamber; fans circulate air through unit 254 nm UV-C	18.6	5	5	8.2 +/- 0.0	7.3 ± 0.3	NA
		37.2		10		6.9 ± 0.1	NA
		55.8		15		6.5 ± 0.2	NA
		12.9	10	5		7.6 ± 0.2	NA
		25.7		10		7.2 ± 0.3	NA
		38.6		15		7.0 ± 0.1	NA
		10.6	15	5		7.8 ± 0.1	NA
		21.1		10		7.4 ± 0.3	NA
		31.7		15		7.1 ± 0.2	NA
Wall-mounted Prototype A: Modified	KrCl/Excimer lamp within enclosed chamber; fans circulate air through unit 222 nm UV-C	15.2	4	5	8.2 +/- 0.1	NA	2.7 ± 1.4
		30.5		10		NA	1.8 ± 0.7
		45.8		15		NA	1.6 ± 1.6
		6.9	10	5		NA	6.0 ± 0.5
		13.7		10		NA	3.5 ± 1.5
		20.6		15		NA	1.4 ± 0.4
		3.4	20	5		NA	6.8 ± 0.3
		6.8		10		NA	5.7 ± 0.7
		10.2		15		NA	4.1 ± 1.3
Wall-mounted Prototype B: Original	Hg bulb within open sconce; fans circulate air through unit 254 nm UV-C	29.9	5	5	8.2 +/- 0.0	6.7 ± 0.1	NA
		59.8		10		5.7 ± 0.2	NA
		89.7		15		4.8 ± 0.3	NA
		15.8	10	5		7.1 ± 0.2	NA
		31.6		10		6.5 ± 0.2	NA
		47.4		15		5.9 ± 0.3	NA
		9.9	15	5		7.5 ± 0.2	NA
		19.7		10		6.9 ± 0.4	NA
		29.6		15		6.7 ± 0.2	NA
Wall-mounted Prototype B:: Modified	KrCl/Excimer lamp within open sconce; fans circulate air through unit 222 nm UV-C	15.6	5	5	8.1 +/- 0.3	7.6 ± 0.1	NA
		31.2		10		7.2 ± 0.4	NA
		46.8		15		6.9 ± 0.6	NA
		7.5	15	5		7.6 ± 0.2	NA
		15.0		10		7.6 ± 0.6	NA
		22.5		15		7.2 ± 0.1	NA
		2.8	30.5	5		8.1 ± 0.1	NA
		5.6		10		7.9 ± 0.2	NA
		8.4		15		7.9 ± 0.2	NA
		0.2	61	5		8.1 ± 0.2	NA
		0.3		10		8.1 ± 0.2	NA
		0.5		15		8.0 ± 0.1	NA
		0.1	71	5		8.1 ± 0.1	NA
		0.2		10		8.1 ± 0.1	NA
		0.3		15		8.1 ± 0.2	NA
Wall-mounted Prototype C	Hg bulb within open sconce; fans circulate air through unit 254 nm UV-C	16.6	5	5	8.2 +/- 0.0	7.4 ± 0.3	NA
		33.2		10		6.7 ± 0.1	NA
		49.8		15		6.1 ± 0.3	NA
		9.1	10	5		7.5 ± 0.2	NA
		18.2		10		7.3 ± 0.2	NA
		27.3		15		6.9 ± 0.2	NA
		6.4	15	5		7.7 ± 0.1	NA
		12.8		10		7.4 ± 0.1	NA
		19.2		15		7.1 ± 0.1	NA

994